UNIVERZITA KARLOVA V PRAZE

Přírodovědecká fakulta

Katedra aplikované geoinformatiky a kartografie

USING SAR DATA FOR WET SNOW MONITORING

ZJIŠŤOVÁNÍ MOKRÉHO SNĚHU Z RADAROVÝCH DAT

Diplomová práce

Jiří Matyáš

srpen 2013

Vedoucí diplomové práce: Doc. Ing. Jan Kolář, CSc.

Vysoká škola: Univerzita Karlova v Praze **Fakulta:** Přírodovědecká

Katedra: Aplikované geoinformatiky a kartografie **Školní rok:** 2012/2013

Zadání diplomové práce

pro Jiřího Matyáše

obor Kartografie a geoinformatika

Název tématu: Zjišťování mokrého sněhu z radarových dat

Zásady pro vypracování

Cílem předkládané diplomové práce je prostudovat algoritmy používané pro zjišťování vlhkého sněhu z radarových snímků, a z těchto algoritmů jeden vybrat a otestovat. Pro realizaci tohoto úkolu bude třeba také vybrat vhodné území a snímky, na nichž bude vybraný algoritmus testován. Hlavní částí práce bude navrhnout úpravu nebo rozšíření vybrané metody tak, aby poskytovala lepší

výsledky. Výsledky získané upravenou metodou na testovacím území budou porovnány s pozemními daty. Práce bude zpracována v anglickém jazyce.

Rozsah průvodní zprávy: cca 30 stran

Vedoucí diplomové práce: Doc. Ing. Jan Kolář, CSc.

Konzultant diplomové práce:

Datum zadání diplomové práce: 26.2.2013

Termín odevzdání diplomové práce: srpen 2013

Platnost tohoto zadání je po dobu jednoho akademického roku.

……	.....……
Doc. Ing. Jan Kolář, CSc.	Ing. Markéta Potůčková, Ph.D.
Vedoucí diplomové práce	Vedoucí katedry

V Praze dne: 26.2.2013

Prohlašuji, že jsem tuto diplomovou práci vypracoval samostatně a že jsem všechny použité prameny řádně citoval.

Jsem si vědom toho, že případné použití výsledků, získaných v této práci, mimo Univerzitu Karlovu v Praze je možné pouze po písemném souhlasu této univerzity.

Svoluji k zapůjčení této práce pro studijní účely a souhlasím s tím, aby byla řádně vedena v evidenci vypůjčovatelů.

V Pardubicích dne 16.8.2013 ……

Jiří Matyáš

Poděkování

Na tomto místě bych rád poděkoval vedoucímu práce, Doc. Ing. Janu Kolářovi, CSc. za čas strávený při konzultacích, trpělivost a cenné rady. Dále bych chtěl poděkovat zaměstnancům Norského ředitelství pro vodní toky a energii, zejména Tuomo Salorantovi, za konzultace ohledně použití jejich dat. Poděkování patří také mým rodičům a mé přítelkyni za podporu a trpělivost v průběhu psaní této práce i celého studia.

Using SAR data for wet snow monitoring

Abstract

This paper focuses on an existing method of snow information retrieval by means of satellite SAR data. The method was first presented by Malnes and Guneriussen (2002), and has been proven to be capable of sub-pixel classification of wet snow. It is also able to classify dry snow pixels. The classification is based on change detection, so a snow-free reference image is required. Some flaws in this algorithm have been discovered during the work on this paper and are discussed, as well as a possible solution is suggested. Because this method is uncapable of classifying pixels containing water bodies, I have proposed an algorithm that can classify snow cover on lakes to enhance its capabilities. Also, a way to improve the wet snow cover classification by means of optical data was suggested.

Keywords: SAR, snow cover, remote sensing, wet snow

Zjišťování mokrého sněhu z radarových dat

Abstrakt

Tato práce se zaměřuje na existující metodu pro získávání informací o sněhové pokrývce z družicových radarových dat. Zkoumaná metoda byla navržena Malnesem a Guneriussenem (2002) a je schopná provést subpixelovou klasifikaci mokrého sněhu, a také klasifikovat pixely se suchým sněhem. Klasifikace je založená na detekci změn, takže je potřeba referenční snímek bez sněhové pokrývky. V průběhu zpracování byly v algoritmu objeveny některé nedostatky, které jsou v práci diskutovány, a zároveň je navrženo možné řešení. Protože tato metoda není schopná klasifikovat pixely ležící na vodních plochách, navrhnul jsem algoritmus, který klasifikuje sněhovou pokrývka na vodních plochách. Zároveň byl navržen možný způsob vylepšení celkové přesnosti klasifikace s využitím optických dat.

Klíčová slova: SAR, sněhová pokrývka, dálkový průzkum Země, mokrý sníh

Contents

ABBREVIATION LISTING

DEM	Digital Elevation Model
EEA	European Environment Agency
ESA	European Space Agency
CORINE	Coordination of Information on the Environment
IR	Infrared
NIR	Near Infrared
NVE	Norges vassdrags- og energidirektorat (Norwegian Water Resources and Energy Directorate)
SAR	Synthetic Aperture Radar
SCA	Snow Covered Area

FIGURE LISTING

TABLE LISTING

CHAPTER 1

Introduction

Using remote sensing techniques for snow observing is useful in hydrological modelling, but also in many other fields. For example the influence of snow covered area and snow properties on animal migration, the animals' condition in spring or condition of vegetation after snow melt can be studied. The biggest advantage of remote sensing is that it allows gathering information from a large area relatively fast and cheap, compared to more traditional land-based methods.

However, the most important use of snow observing is snow melt and runoff modelling. Information about snow is a valuable variable in most runoff models. Outputs from such models may help predict increased flood risk, furthermore, spring floods from melting snow are especially difficult to predict. For example, in 1995 the Østland region in southern Norway was struck by one of the strongest floods ever recorded in this part of the country. It was also thanks to remote sensing data that the unusually long-lasting snow cover was discovered, which helped predict the flood and decrease the damage it caused (Moen and Landmark, 2008).

This kind of information is also very important in the hydropower industry. In Norway 98 % of all power comes from hydroelectricity plants (Storvold et al., 2006), while around half of the annual precipitation in Norway comes in the form of snow (Rognes et al., 2005). A majority of Norwegian hydro plants lies in high altitudes and their catchments often cover vast mountainous areas, where regular land-based measurements would be complicated and costly. Knowledge of the amount of water stored in the form of snow, together with the speed of snow melt, is essential to efficiently manage the water level in the reservoir to prevent overflowing or shortage of water. The amount of water stored as snow can also significantly influence the prices of electricity throughout the year (Rognes et al., 2005). For the reasons given in this chapter, most power companies are constantly developing and improving their own runoff models to gain access to the most

precise predictions possible. For remote sensing data to be useful in such models, they should not differ from reality by more than 10 % (Storvold et al., 2006).

In this paper, existing methods for deriving snow covered area (SCA) from remote sensing data will be described. I will focus mainly on the use of radar instruments, which have repeatedly been used in methods that had promising results, not only for SCA monitoring, but also for monitoring other snow properties, mainly its water equivalent. Unlike the instruments that operate in the visible or infrared (IR) part of the electromagnetic spectre, radar device have a big advantage in being able to operate nearly in all meteorological conditions and gathering information at night or through clouds. In Norway cloud cover is very common during winter, so radar instruments can provide information much more frequently than instruments operating in other parts of the electromagnetic spectre, which would be often obstructed by clouds. Another advantage of radar systems is that radar waves can penetrate relatively deep under the surface of snow. Thus information from below the snow surface can be gathered, which can help understand the snowpack's properties better.

I will then choose one of the presented methods and apply it on a remote sensing data set to gather information about the extent of wet and dry snow. This method's properties, advantages and disadvantages, possibilities of operational use and possible potential for improvement will be discussed. Details about the test data and area of interest will be given further in this paper.

CHAPTER 2

Microwave and radar sensors

Microwave sensors detect radiation of wavelength from about one millimeter up to nearly one meter. The main advantage of using microwave sensors for remote sensing is the ability to penetrate cloud cover, rain or fog and they are independent of light conditions, which means they can operate during day as well as at night. However, the radiation intensity of most natural objects on these wavelengths is very low, so data gathered by passive microwave sensors suffer from poor spatial resolution. The reason for this is that for the radiation to be detectable, it must be gathered from a relatively large area.

Radar devices possess the advantages of microwave sensors. In addition, they are equipped with their own source of radiation, so they are not dependent on the intensity of passive radiation of surfaces and therefore can gain a much better spatial resolution. The sensor then records the so-called echo – the strength and form of the backscattered signal. The echo contains information about some physical properties of the scatterer. By measuring the time lag between transmitting and receiving the signal, the distance between the radar and the object can be measured.

2.1 Imaging radar principle

The principle of imaging radar is depicted on figure 1. Radar transmits the signal a little sideways, instead of directly beneath itself. It is important for the radar instrument to be able to determine, where did the backscattered signal come from. Otherwise, backscattered signal from places that lie in the same distance but opposite direction from the nadir would reach the sensor at the same moment and the sensor would not be able to determine which side of the nadir, did the respective backscatters come from. The side-looking principle also allows achieving better ground range resolution. The angle between the radar antenna and the nadir is called look angle, or off-nadir angle and commonly lies between 20

and 50 degrees. The angle at which the signal reaches the ground is slightly higher due to Earth's curvature. The ERS satellite's look angle is 21 degrees and the signal reaches the ground at an angle of 23 degrees (Ferretti et al., 2007).

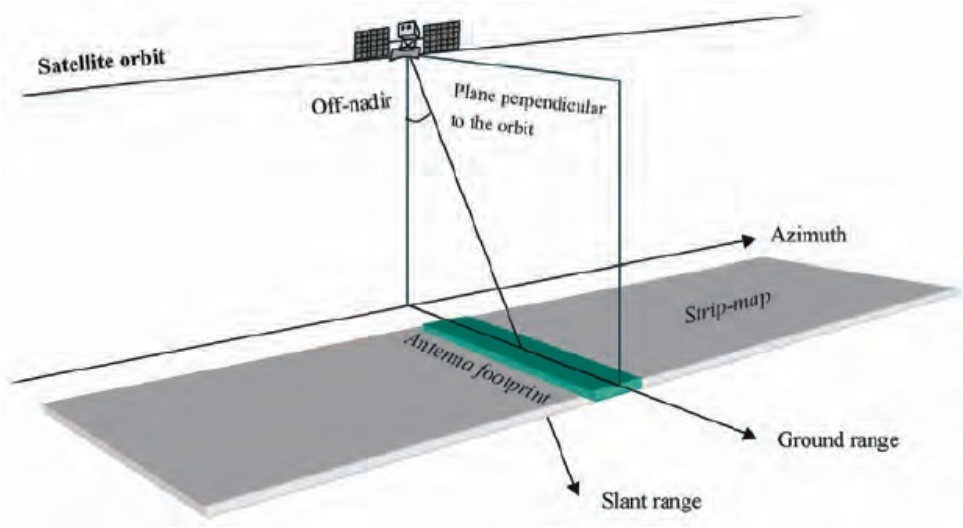

Figure 1:The principle of imaging radar (Ferretti et al., 2007).

Azimuth resolution can be calculated by equation 1 where R_a is azimuth resolution, h is the satellite's height above the terrain, λ is wavelength, L antenna length and θ is the angle at which the signal reaches the ground, or incidence angle (Elachi, 1998 in Finsland, 2007).

$$\mathbf{1}: R_a = \frac{h * \lambda}{L * cos\theta}$$

In case of instruments on the Earth's orbit, their height above terrain is very high. From equation 1 we can see that this leads to either poor azimuth resolution or the need to use a very long antenna or short wavelengths. Shorter wavelengths are, however, more significantly influenced by the Earth's atmosphere and constructing a very long antenna brings some engineering issues. This is why synthetic aperture radars, or SARs, are used.

2.2 Synthetic aperture radar

Synthetic aperture radar (SAR) is a radar system that takes advantage of the Doppler-effect to simulate a longer antenna and improve azimuth resolution. The satellite moves relatively to the terrain, which leads to a change of the

backscattered signal's frequency dependent on the speed and direction of the movement related to the scatterer (pixel). The radar signal backscattered from a pixel is being recorded for a certain period of time that depends on the width of the radar beam. During this time period the backscattered signal is being recorded and is further processed as if it was recorder by an antenna with length equal to the distance the satellite has travelled while recording the signal.

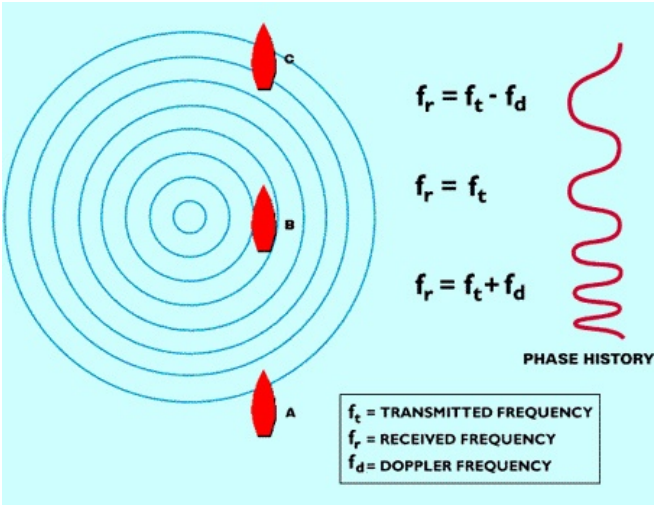

Figure 2: Doppler-effect. Source: ESA (c2013)

The principle of the Doppler-effect is shown on figure 2. In position A the receiver is nearing the transmitter and receives a signal with a higher frequency than the transmitted signal. In position B the received frequency is equal to transmitted frequency while in position C the receiver is moving away from the transmitter, which causes the received frequency to be lower than transmitted. In the right part of the image there is a curve that shows a possible history of the received signal's frequency.

Figure 3 shows how the Doppler-effect relates to SAR. Backscattering from areas b and c will have lower and higher frequency than transmitted respectively, while in case of backscattering from area a there will be no change in frequency. If we imagine the instrument moving forward, signal backscattered from area a would have a lower frequency and backscattering frequency from area c would not be changed.

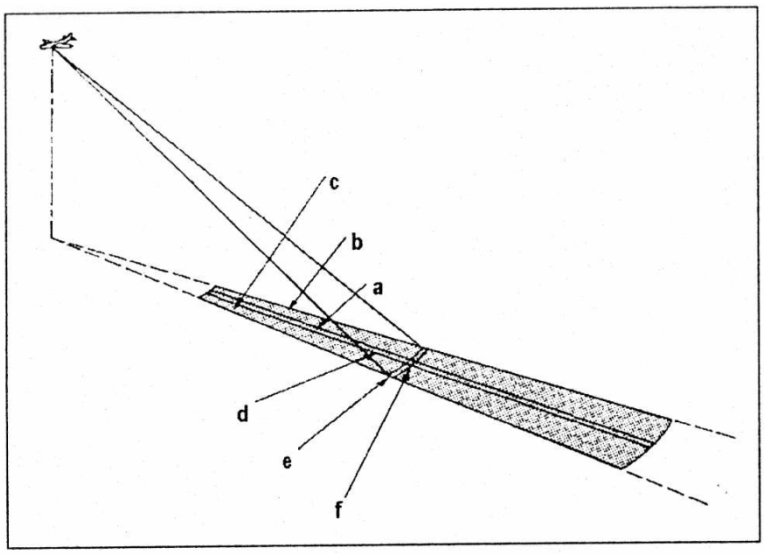

Figure 3: Relation of SAR and the Doppler-effect. a – zero frequency shift, b, c – lower and higher frequency respectively, d – azimuth resolution, e – ground range resolution, f – Resulting pixel. Source: Dobrovolný (1998).

2.3 SAR images geometry and topographic effects

As shown in figure 1, the distance between the radar and an imaged object can be represented in two different ways. Either as slant range, which is the direct distance between the two objects, or as ground range, which is the distance between nadir and the imaged object. An object's (pixel's) location on a radar image is determined by the time of receiving backscattered signal. This means that a radar is determining the pixels' position by slant range, but slant range distorts ground range scale – the scale increases with increasing slant range. Slant range can be converted to ground range using the Pythagorean theorem, but such procedure assumes flat terrain (Dobrovolný, 1998).

$$\mathbf{2}: \Delta g = \frac{\Delta H}{tg\theta}$$

Moreover, a hilly terrain causes further distortions, which are more difficult to correct and require a digital elevation model (DEM). Foreshortening occurs, when the terrain is sloped against the instrument. It causes slopes on the image to appear shorter than they actually are. In figure 4, the distance of AC is equal to that of AD, but the slant range recorded by SAR shows A'D' significantly shorter than A'C'. The reason is, that backscattered signal from point D reaches the sensor sooner than signal backscattered from C, because D is much closer to the sensor

than C. To correct foreshortening we need to know the elevation difference *ΔH*, and incidence angle θ. The shift in the point's position is than calculated according to equation 2 (Finsland, 2007).

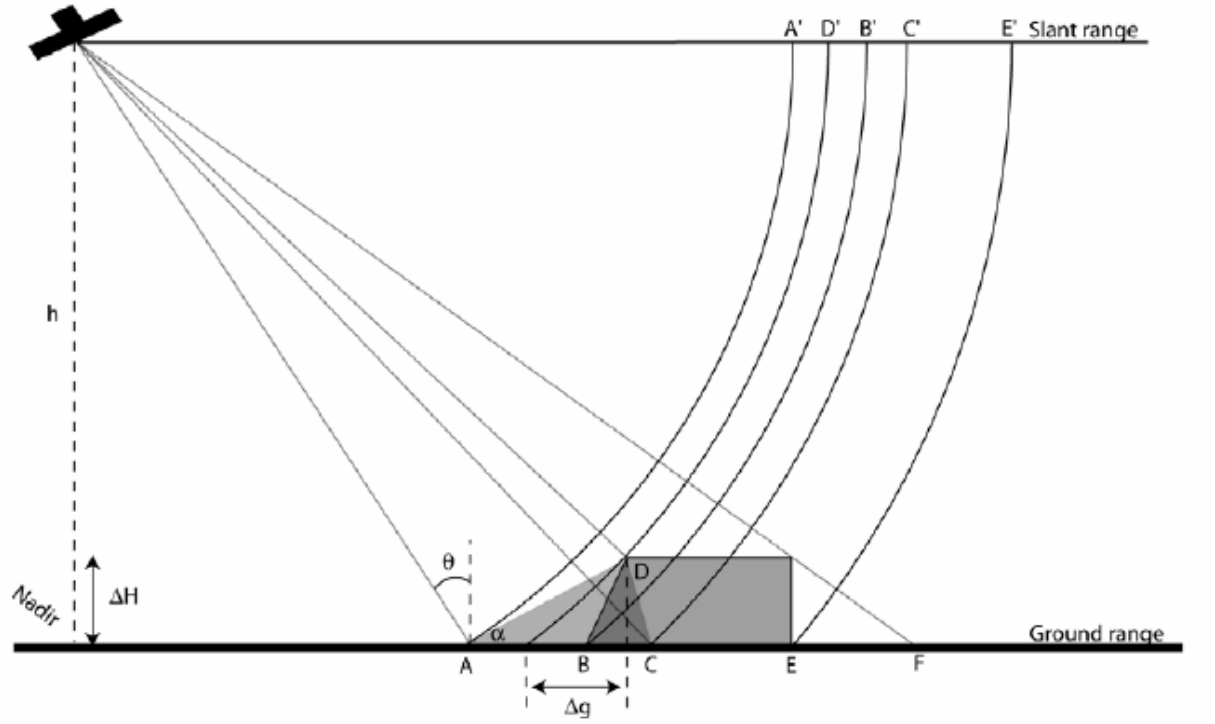

Figure 4: Distortions caused by terrain. Source: Finsland (2007)

Layover occurs when a hill's slope α exceeds the look angle and the slope is turned towards the sensor. If the slope is turned away from the sensor, shadow occurs instead. In case of layover, a mountain top appears before the mountain's foot in the image. This is also shown on figure 4 – D' appears before B', even though B is closer to nadir than D. Backscattering from certain parts of the slope will be melted together and no useful information will be gained from these parts. If a hill's slope was equal to the look angle, backscattering from the entire slope would be recorded at the same moment and the entire slope would be shown as a single pixel with very high backscattering intensity. SAR does not receive any information from areas influenced by shadow, because the radar signal cannot reach these areas at all. In figure 4, shadow occurs between E and F (Finsland, 2007).

2.4 Radar signal properties

Parameters of a backscattered radar signal can be divided into two categories – inner parameters, or parameters that are influenced by the radar itself and outer

parameters, or parameters influenced by the scatterers. Typical inner parameters are wavelength, signal polarization or look angle. Outer parameters are surface roughness (related to local incidence angle), wetness, topography or the surface's dielectric properties (Dobrovolný, 1998). Topographic effects have been described in the previous chapter.

2.4.1 Inner properties

Table 1 shows the wavelengths and names for the most common radar bands. Wavelength is an important factor that determines the signal's ability to penetrate atmosphere, soil or snow cover. Shorter wavelengths below 3 cm are more influenced by the atmosphere and also have smaller capabilities in penetrating soil and snowpack (Dobrovolný, 1998). Currently, satellite systems operating in bands C (ERS), X (TerraSAR-X) and L (JERS) are active.

Band	Wavelength [cm]	Frequency [MHz]
Ka	0,75 – 1,1	40 000 – 26 500
K	1,1 – 1,67	26 500 – 18 000
Ku	1,67 – 2,4	18 000 – 12 500
X	2,4 – 3,75	12 500 – 8 000
C	3,75 – 7,5	8 000 – 4 000
S	7,5 – 15	4 000 – 2 000
L	15 – 30	2 000 – 1000
P	30 - 100	1 000 - 300

Table 1: Radar bands, according to Dobrovolný (1998).

Radar signal can be polarized. If a signal is not polarized, the wave oscillates in all directions, otherwise only in one plane perpendicular to the signal's direction. Transmitted signal can be polarized either in vertical (V) or horizontal (H) plane. Also the received signal can be polarized, which means that a radar signal can be transmitted and received in total four different regimes. Either identical (HH and VV) or unlike (HV and VH) polarization can be used. Signal polarization can be used to gather information about so-called depolarizing surfaces. While comparing

two images with different polarization such a surface would appear different in each image (Dobrovolný, 1998).

Incidence angle has a significant influence on topographic distortions. Large incidence angles cause topographic distortions more often, because a less steep slope is needed for a topographic effect to occur with large incidence angle. Larger incidence angles also make it harder for the signal to penetrate vegetation. At the same time, by increasing incidence angle stronger backscattering from rough surfaces can be achieved (Dobrovolný, 1998).

2.4.2 Outer properties

Radar signal received from a single pixel usually comes from more than one scatterer. In some cases however, a scatterer may cause such an intensive backscatter, that it makes backscattering from all other scatterers in the pixel insignificant and this backscatter will be recorded in the image. A typical example is the corner of a building, which may cause backscatter of nearly all transmitted signal back to the radar (figure 6c). Figure 5 shows a trihedral corner reflector. Despite its relatively small surface, such a reflector will be very well visible on the radar image, because it will return almost all the transmitted signal back to the radar. Unlike a corner of a building, where the reflector is only dihedral, it is less sensitive to the direction from which the signal comes (Finsland, 2007). Trihedral corner reflectors have been used for image calibration and geocoding by, among others, Malnes et al. (2004).

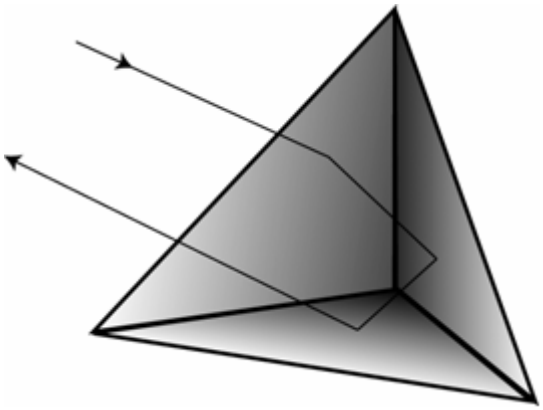

Figure 5: A trihedral corner reflector. Source: Finsland (2007)

Backscattering intensity is a very complex topic and depends on wavelength, polarization, local incidence angle and dielectric and geometric

properties of the surface. Different kinds of backscattering depending on surface roughness are shown in figure 6. In part a, diffusive backscatter is shown, in part b mirror reflection and in part c corner reflection. Whether or not a diffusive backscatter will occur depends on the surface roughness. Surface roughness is defined relative to wavelength and local incidence angle (Dobrovolný, 1998). According to Kolář et al. (1997), surface roughness is determined by the Rayleigh criterion. An object is considered a diffusive scatterer if formula 3 is true. In formula 3, *rms* is the square root of the unevenness height squared, λ is wavelength and θ is local incidence angle.

$$\mathbf{3}: rms > \frac{\lambda}{8 * cos\theta}$$

Kolář et al. (1997) consider a surface as a mirror reflector when formula 3 with flipped inequality sign applies. Other authors, for example Dallemand (1993, in Dobrovolný, 1998) relate surface roughness towards average unevenness height.

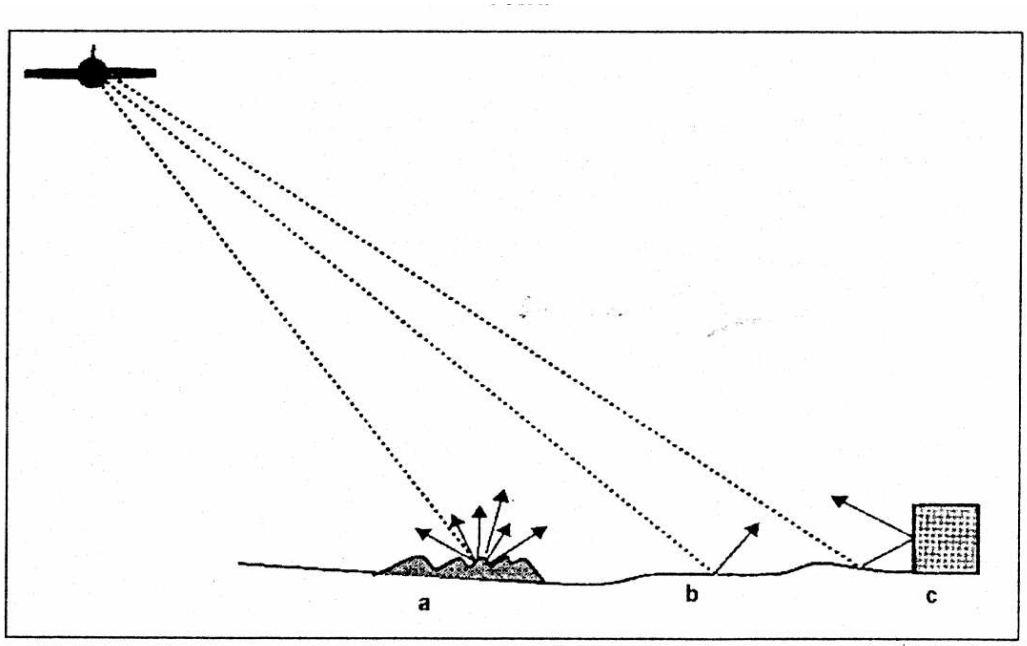

Figure 6: Reflection types depending on surface roughness. Source: Dobrovolný (1998)

By surface roughness we may define three different types of scatterers. Diffusive scatterers scatter the signal in all directions, and a part of the scattered signal is recorded by the sensor. Smooth reflectors reflect most of the signal away from the sensor and no or very little backscatter is recorded. Orientation of the surface to the radar beam also plays an important role. Smooth surfaces that are perpendicular to the radar beam will reflect nearly all of the radar signal back to the

sensor, which will result in a bright point on the image. Other surfaces with the same roughness but different orientation would, on the other hand, appear as dark points on the image, because most of the signal would be reflected away from the sensor. Corner reflectors are the most common in cities. But even here, orientation of the surface to the sensor plays an important role. Equally rough or smooth surfaces may therefore result in different backscattering intensity depending on the local incidence angle (Dobrovolný, 1998).

Dielectric properties characterize a material's ability to reflect, conduct or absorb electromagnetic energy. To describe them, the dielectric constant is used. Generally we can say that the dielectric constant is proportional to the backscatter intensity. Dielectric constant is however also proportional to the amount of water contained in the material. Most commonly, the dielectric constant ranges from 3 to 8, but the dielectric constant of water is 80. Changes in backscattering intensity may therefore be related to change of water content in the object, rather than to other changes in the object (Dobrovolný, 1998).

CHAPTER 3

Snow characteristics and measurement

3.1 Snow formation

When the atmosphere is saturated with water vapour or when air temperature drops below dew point, water vapour in the atmosphere condenses. If the temperature is lower than 0°C, deposition occurs instead. This means that water transitions from gaseous state directly to solid state. This process is sometimes also called crystallization. Gaseous water is deposited in solid (frozen) state on small solid objects contained in the atmosphere, for example dust particles. Water molecules are than agglomerated into crystalline formations – snow crystals.

Snow crystals can possess a nearly unlimited range of different shapes and sizes, depending on the amount of gaseous water in the atmosphere or temperature during condensation. At low air temperatures, only single snow crystals are observed, while at temperatures nearing 0°C the snow crystals group together to form snowflakes - the higher the temperature the bigger the snowflakes (Doležal and Pollak, 2004).

3.2 Types of snow

Snow cover can be classified in several different ways. Most commonly it is categorized according to its texture, grain size and wetness.

If snow is categorized according to its texture, criteria like grain size and shape, snow pack compactness or pore size are taken into account. All of these are dependent on the age of snow and on meteorological conditions. Freshly fallen snow is not compact and is the foundation for powder avalanches (Finsland, 2007). It is also easily transported by wind. This type of snow is called fresh or powdery. When fresh snow gets more compact, e.g. because of wind or its own weight, it

becomes crud. Crud is the foundation for slab avalanches (Finsland, 2007). Snow particles in crud are called decomposing or fragmented particles. Granular snow is snow that has been lying for a long time. It can be further categorized according to grain shape as either snow with rounded grains or solid faceted crystals. Last but not least, firn is the type of snow that has been lying for a very long time (most commonly over a year, but sometimes even the last remnants of spring snow are categorized as firn). Firn has often large round grains and the original snow crystal has been completely metamorphosed (Doležal and Pollak, 2004).

Category	Grain size [mm]
Very fine grains	<0.2
Fine grains	0.2 – 0.5
Medium grains	0.5 – 1.0
Coarse grains	1.0 – 2.0
Very coarse grains	2.50 – 5.0
Extremely coarse grains	> 5.0

Table 2: Snow grain size classification according to Doležal and Pollak (2004).

Snow classification by grain size according to Doležal and Pollak (2004) is shown in table 2 while table 3 shows the same author's way of classifying snow according to its wetness, or liquid water content.

Category	Average liquid water content [%]
Dry snow	0
Moist snow	< 3
Wet snow	3 – 8
Very wet snow	8 – 15
Extremely wet snow	> 15

Table 3: Snow wetness classification according to Doležal and Pollak (2004).

3.3 Land-based measurements of snow characteristics

Snow depth, grain size, or snow water equivalent are among the most commonly measured snow properties. Furthermore, analysis of snowpack stratification is often performed in order to evaluate the snowpack's stability and avalanche risk. Snow water equivalent is usually presented in millimeters and describes the depth of water that would result from melting of all snow over an area of one squared meter. It is likely to be the most valuable variable that can be used in snowmelt and runoff modelling, because it states exactly how much water is stored inside the snowpack.

The traditional measurement techniques are rather simple. Depth is simply measured by a long probe. For measuring water equivalent, one first takes a snow sample of known volume. For gathering such a sample, NVE (2008) recommends using a one meter long metal (preferably steel or aluminium) cylinder with a diameter of ten centimeters and sharp edges on its lower side, to cut through snow easily. A hole in the snowpack (all the way to bare ground) is dug to allow easier manipulation with the cylinder. A sample is than taken with the cylinder by the edge of the hole. If the snow is deeper than the cylinder, samples are taken until one reaches the ground. For each sample we measure its weight and if the cylinder is not full (in case of the last sample before reaching bare ground) also its volume is measured. From these measurements one can easily compute the snow's density and using snow depth also snow water equivalent.

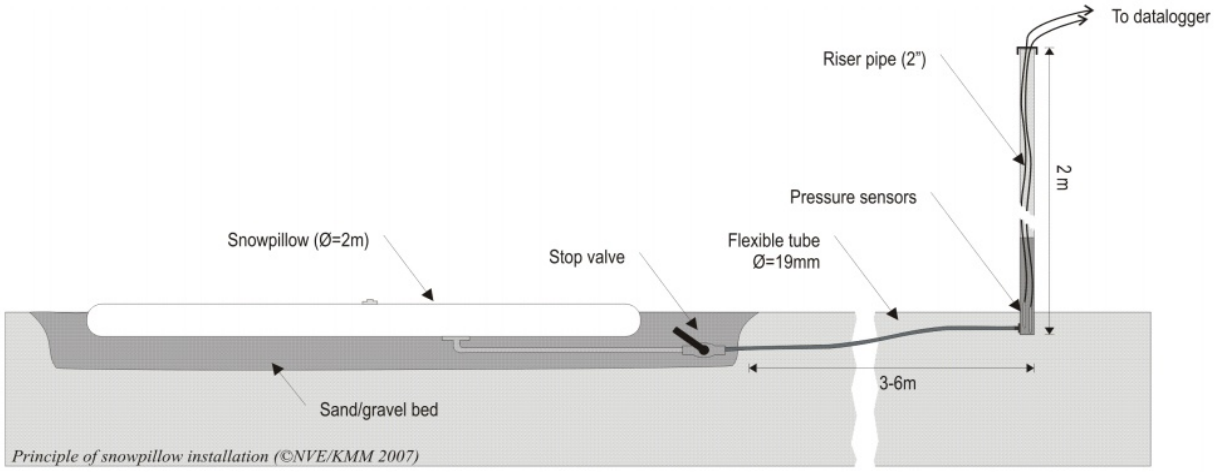

Figure 7: The principle of snowpillows. Source: NVE (c2007)

For automatic measurements of snow water equivalents, so called snowpillows are used. These pillows measure the weight of snow from which its water equivalent is computed. The way such devices work is shown on picture 7. Unfortunately, these devices are not cheap, so automatic snow water equivalent measurements in Norway are only performed by 25 snowpillows.

3.4 Remote sensing-based retrieval of snow properties

Land-based methods for measurement of snow properties are precise, but have several disadvantages. Automatic measurement devices are expensive, manual measurements are time-consuming and they are not exactly cheap either. Besides, all of the land-based methods only provide information from a single point, and to get areal data, these point measurements must be interpolated; and interpolation techniques are burdened with errors.

As mentioned before in this paper, remote sensing can be used to gather information over a large area fast, relatively cheap and without interpolation errors. However, interpreting the information collected by remote sensing techniques is tricky and requires an intensive research.

The Norwegian Water Resources and Energy Directorate (Norges vassdrags- og energidirektorat, NVE) currently uses NOAA (National Oceanic and Atmospheric Administration) AVHRR (Advanced Very High Resolution Radiometer) images operationally to retrieve snow covered area (SCA). This system has been in operational use since mid 1990s, while the first attempts to retrieve snow information by means of remote sensing began in 1978 (NVE, 2009). This system, however, cannot retrieve information through cloud cover. Such a limitation poses a big problem, because cloud cover is a common phenomenon in Norway, especially during winter. And like this system, all sensors operating in visible or IR part of the spectre are good in retrieving SCA, with some limitations even distinguishing wet and dry snow, but their operational use is strongly limited by the requirement of daylight or cloud-free conditions.

Snow water equivalent (SWE) has been attempted to be measured with SAR, with promising results. The delta-k technique, first presented by Engen et al. (2003), has shown promising results. However this method has several drawbacks that would make its operational use very complicated. Some of these drawbacks

are the possibility of measuring only dry snow's SWE, the need for precise calibration and deployment of corner reflectors in the area or the need to average to larger pixel size, which results in a rather poor spatial resolution. Furthermore, current satellite-borne SAR instruments are far from ideal for SWE monitoring and using other bands, like Ku-band, (or even multiple bands) has been suggested in order to improve the results. However, it seems unlikely that a new SAR instrument with specifications better for SWE monitoring would be launched any time soon, so finding a better SWE retrieval algorithm for C-band SAR is currently the best way to make progress in this area.

SAR instruments have however been used a bit more successful in retrieving SCA, especially wet-snow cover, and some operational algorithms have already been developed (see for example Nagler and Rott, 2000). However, these algorithms are still far from perfect. The biggest flaw in using SAR for snow monitoring is the fact, that on SAR images it is impossible to distinguish dry snow from snow-free ground (Koskinen, 2001) so alternative methods are used to retrieve dry-snow covered area, such as assuming that all pixels that have not been classified as wet snow and lie above the average (or median) altitude of pixels classified as wet snow are dry snow. Surprisingly enough, such techniques perform quite well. The SCA retrieval algorithms will be discussed more thoroughly in the Methods chapter.

Property	**Visible/NIR**	**IR**	**Microwave**
Snow extent (SCA)	Yes	Yes	Yes
SWE	Fair *(shallow snow only)*	Poor	Fair
All weather capability	No	No	Yes
Spatial Resolution	~10 m	~100 m	*Passive sensors 20 – 150 km* *Active sensors ~30 m*

Table 4: Remote sensing instruments' capabilities in retrieval of some snow properties according to Rango (1986) in Koskinen (2001).

Table 4 summarizes the capabilities of various types of remote sensing instruments in retrieval of snow properties. As was said before, microwave and especially SAR instruments are likely to be the best choice for operational snow

monitoring, because of their good capabilities in retrieving the information, their independence on weather conditions and a reasonable spatial resolution.

3.5 Backscattering from snow-covered terrain on visible, NIR and IR wavelengths

Figure 8 shows the spectral curve for snow. The backscattering, or reflectance, is, however, strongly dependent on other factors, such as water content, grain size or dirt/dust particles content. The backscattering from fresh snow is several times higher than backscattering from older snow. The effect of snow-grain size on backscattering from the snowpack is the strongest in near infrared (NIR) where even a small change in grain-size results in a significant change of backscattering intensity (Kolář et al., 1997). In general, snow has very high backscattering intensity in visible and NIR wavelengths. This is followed by a major drop to near zero backscattering, with the minimum lying around 1.5 μm and 2.0 μm. These characteristics make it easy to distinguish snow from other objects on Earth's surface.

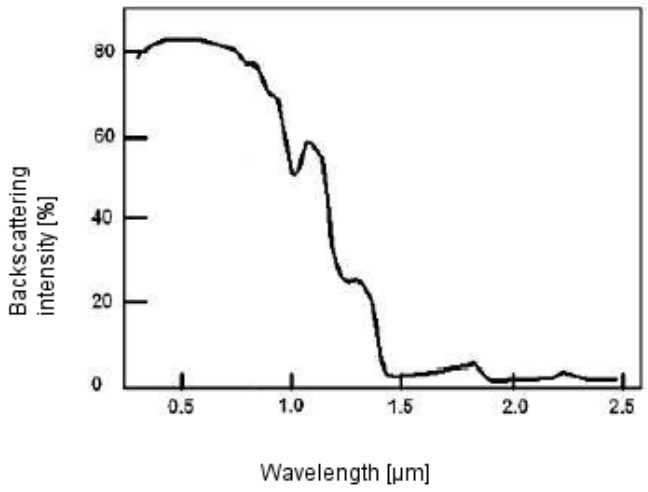

Figure 8: Spectral curve of snow. Source: Zhang (2008) in Špátová (2010)

The spectral curves for multiple types of surfaces are shown in figure 9. It is obvious that snow cover is most easily detected in visible and NIR part of electromagnetic specter, where its reflectance is much higher than the reflectance of any other surface. The only objects that might be easily misclassified as snow are clouds. As seen in figure 10, the backscattering intensity of clouds on visible and NIR wavelengths is very similar to that of snow cover. However, around 1.5 μm

where the reflectance of snow is dropping, the reflectance of clouds remains very high, so these wavelengths should be used for separating cloud cover from snow.

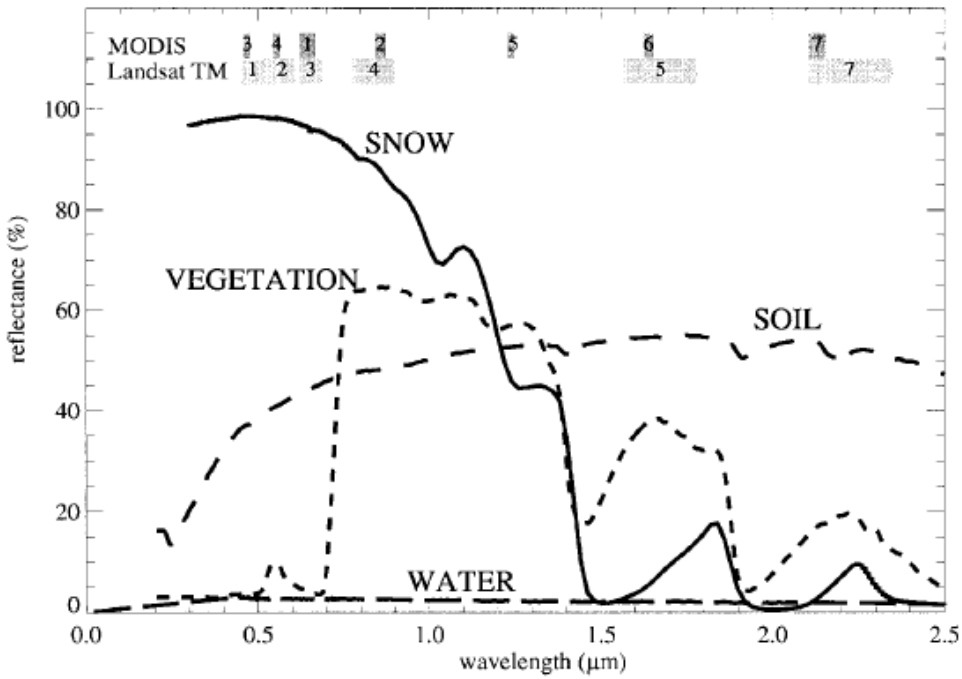

Figure 9: Spectral curves for some of the most common surfaces. Source: Klein et al. (1998)

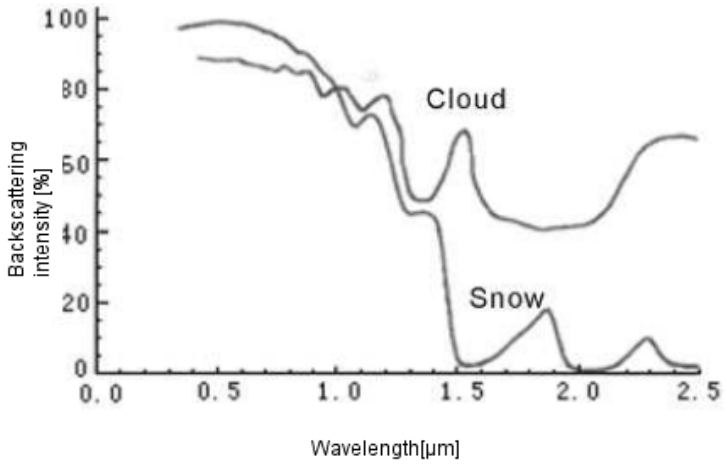

Figure 10: Spectral curves of snow and clouds. Source: Zhang (2008) in Špátová (2010)

3.6 Microwave backscattering from snow-covered terrain

The intensity of backscattering is commonly represented by backscattering coefficient. Backscattering coefficient ρ at wavelength λ is defined as the ratio of backscattered radiation intensity M_r and the intensity of radiation emitted to the

surface M_i. The simple formula for computing backscattering coefficient is given in formula 4.

$$\mathbf{4}: \rho(\lambda) = \frac{M_r(\lambda)}{M_i(\lambda)} * 100$$

Snow backscattering coefficient is a result of the influence of three components. These mechanisms of backscattering for a homogenous layer of snow is depicted in figure 11, A being backscattering from snow-air interface, B volume scattering from the snowpack and C Backscattering from the underlying ground. If the snowpack is not homogenous and consists of more layers, the boundaries between these layers also contribute to backscattering, as well as each layer's volume.

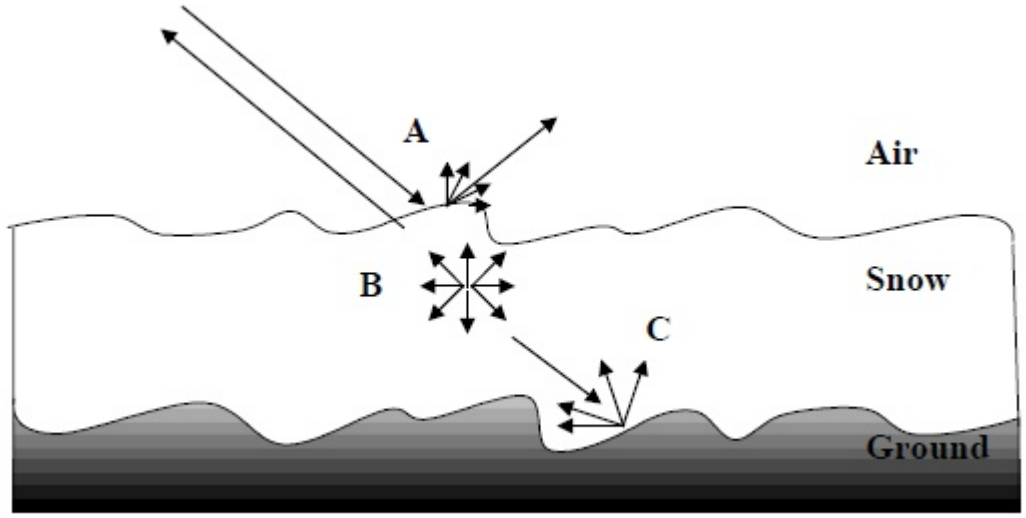

Figure 11: Backscattering mechanism from a homogenous snowpack. Source: Koskinen(2001)

3.6.1 The effect of snow wetness on backscattering

In case of dry snow, the dielectric contrast at the air-snow interface is very low and so is the reflection coefficient. This means that the backscattering from air-snow interface in the case of dry snow could be neglected. Also the volume scattering has low significance, but increases with increasing depth of the snow pack, as the signal is attenuated and the ground's contribution to total backscattering decreases. Furthermore, the low dielectric contrast causes the importance of snow roughness to diminish. The backscattering coefficient of dry snow also decreases with increasing incidence angle. This is caused by decreasing contribution from the ground, as the incidence angle increases. The influence of incidence angle was

computed by Koskinen (2001) using a model by the same author and the result is shown in figure 12. This is important to bear in mind when comparing multiple products with varying incidence angle.

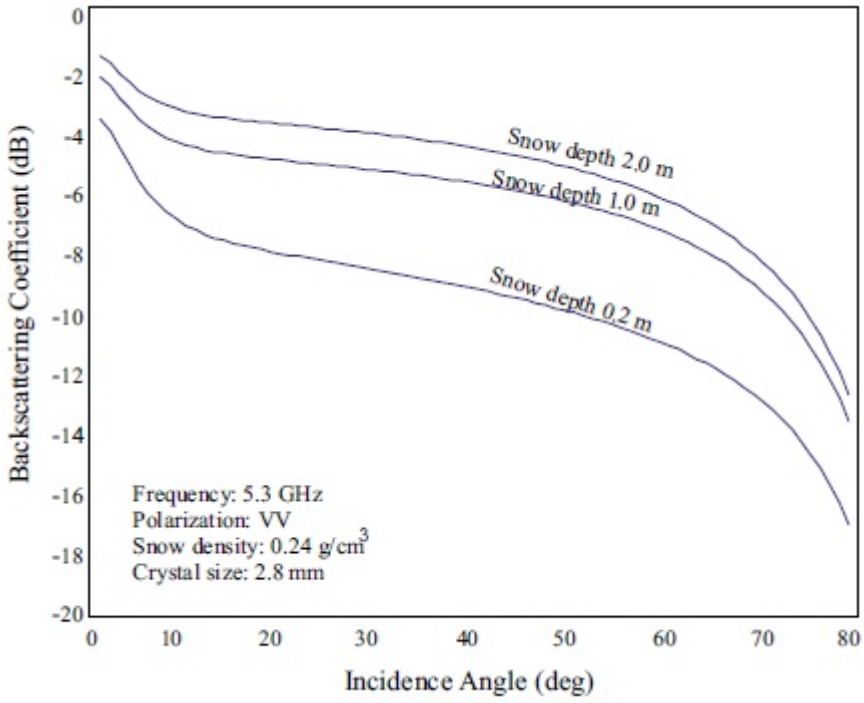

Figure 12: The effect of snow depth on backscattering coefficient as a function of incidence angle. Source: Koskinen (2001).

When the snowpack is wet, the water contained in the snowpack absorbs some of the signal. This is why an increase in snow wetness (also meaning an increase of liquid water content) leads to decreasing contribution of the ground to the total backscattering. The wetter the snowpack, the more radar signal is absorbed and not backscattered. Therefore the total backscattering coefficient decreases with increasing snowpack wetness, which is shown in figure 13. The influence of incidence angle on backscattering as a function of snow wetness has also been modelled in figure 13. The simulation has been performed by Koskinen (2001). Increasing incidence angle leads to a decreasing backscattering coefficient, but the general functional behaviour remains the same for any incidence angle. This means that the backscattering coefficient decreases nearly linearly until 2% of wetness for any incidence angle. After reaching around 2% wetness the curve stops the rapid decrease and levels out.

Snow wetness also causes an increase of the dielectric contrast at the snow-air interface, which results in a higher contribution of this interface to total

backscattering and to increasing significance of surface roughness. In fact, if the snow is wet enough, the surface backscattering may even be the most significant component in total backscattering. Therefore, the snow surface roughness is very important to be accounted for when modelling backscattering of wet snow.

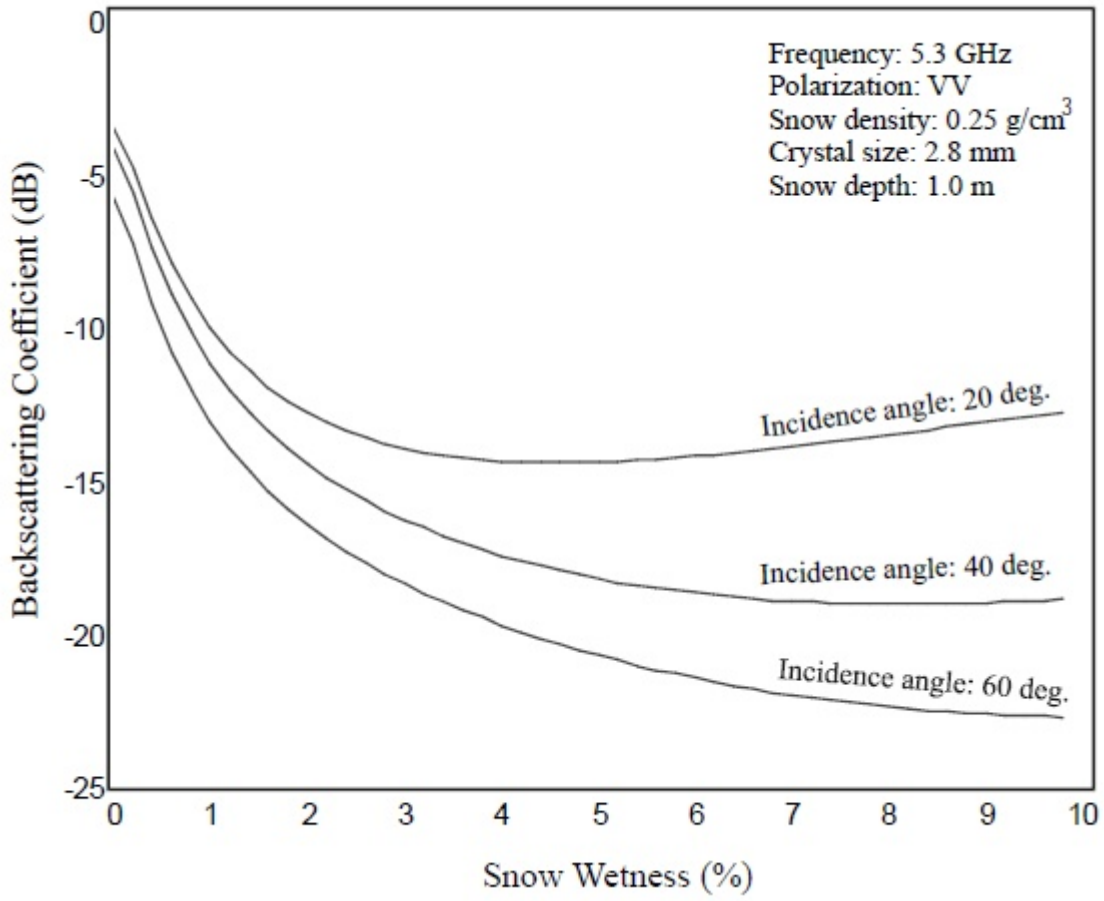

Figure 13: The effect of snow wetness on backscattering coefficient. Modelled by Koskinen(2001).

Figure 14 shows the diurnal behaviour of snow wetness as well as backscattering coefficient on various microwave frequencies. Unlike figures 12 and 13, the data in figure 14 are observed. These observations show that snow wetness may vary significantly throughout the day, depending on changing air temperature or sunshine. Based on the data from figure 14, one should be very careful when interpreting the results of a remote sensing-based snow wetness analysis, because the reference data may have been taken in a different time of the day than the remote sensing images. This must therefore be taken into account when evaluating the results of this paper.

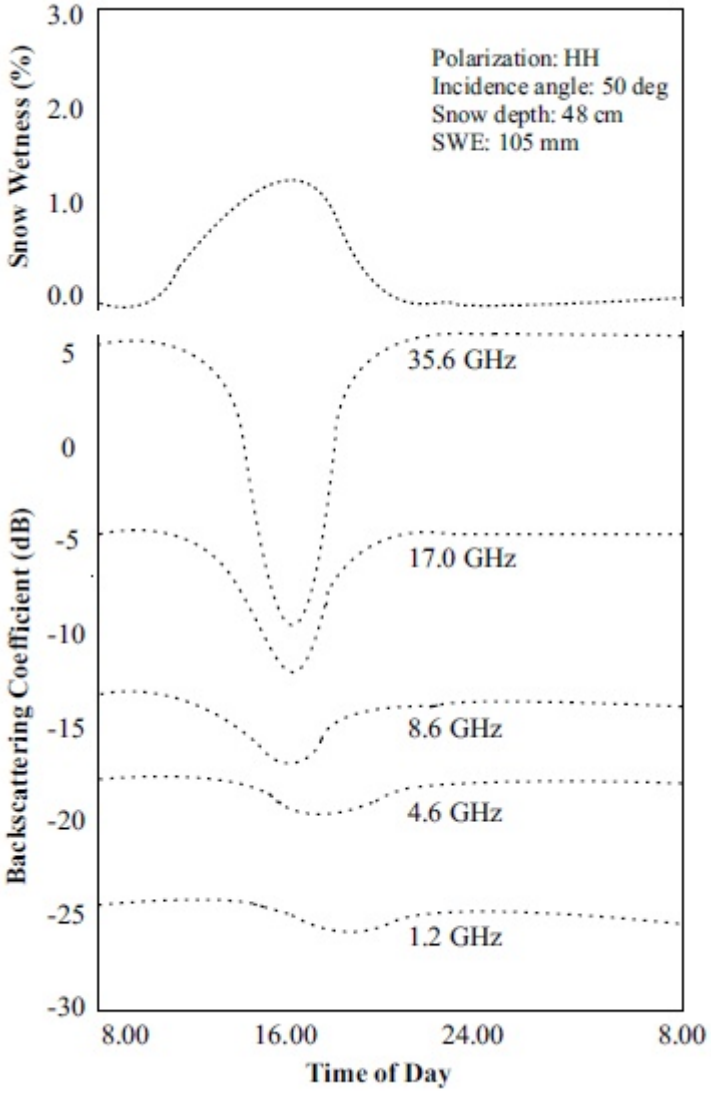

Figure 14: The diurnal pattern of snow wetness and backscattering coefficient. As observed by Koskinen(2001).

From figure 14 we can also see that higher frequencies respond to changes in snow wetness more drastically. This is because high frequencies do not penetrate so deep into the snowpack and the total backscatter is dominated by backscattering from the air-snow interface. High frequencies, like Ku- or K-band, may therefore be useful in monitoring dry snow. A single satellite radar, operating on multiple frequencies and polarizations, could therefore gather information simultaneously from the air-snow interface, the snowpack and the snow-ground interface, because each of these responds to different frequencies. Many authors, like Koskinen (2001), have therefore expressed their hopes for a future multi-channel SAR instrument that would allow better operational snow monitoring. Such an instrument, unfortunately, is unlikely to be launched in the near future, and that

is why it is extremely attractive to try and find an operationally-useable method for snow monitoring using one of the currently operational radar instruments.

We can thus summarize that:

- Wet snow has significantly lower backscattering coefficient than dry snow.
- Dry snow will probably be difficult to distinguish from bare ground, especially on lower frequencies like C-band.
- Each part of the snowpack responds differently to different wavelengths which makes it nearly impossible to gather information about the entire snowpack.
- Most of the backscattering from a wet snowpack comes from the snowpack's volume scattering and the air-snow interface; the signal does not reach the ground in deep snowpack.
- In the case of dry snow, most backscattering comes from the ground and some from the snowpack's volume scattering.
- Snow backscattering coefficient decreases nearly linearly until 2% of snow wetness. The favourable limit for wet snow could therefore be 2% of volumetric wetness.
- The backscattering coefficient is strongly related to the snow's wetness
- Snow wetness, as well as backscattering coefficient, changes significantly throughout the day.
- The total backscattering coefficient changes with incidence angle, but the functional behaviour remains the same.

CHAPTER 4

Data and test area

4.1 The test area

The area upon which I will attempt to observe wet snow cover must satisfy a few requirements in order to provide good conditions for developing and evaluating a SCA retrieval algorithm.

First of all, the terrain should be rather flat. This should help avoid topographic distortions and also the results should be easier to evaluate if pixels contain data from roughly the same altitude (snow properties can vary significantly on short distances if altitude does).

Since it is complicated to retrieve information from forested areas, the test area should contain some open ground or low vegetation. Also bogs or mires could pose a problem, because they are likely to appear as water bodies or wet snow due to the high amount of liquid water contained in them.

Furthermore, it is important to find an area where the snowpack during winter is thick and stable enough so that so that the backscatter actually carries information about the snowpack. The snowpack's stability is important, because repeated freeze-thaw cycles lead to complicated stratification in the snowpack, which makes retrieving the snowpack information a bit more complicated.

Finally, there must be some ground-truth data available in the selected area so that the results can be evaluated.

These requirements are best satisfied in Scandinavian regions. The alpine regions satisfy the requirements of thick and stable snowpack and low or no vegetation, however, the terrain in these regions is so steep that radar instruments

cannot retrieve information from a large area. Eventually I have selected an area in southern Norway. The approximate location of the test area is shown in figure 15.

Figure 15: A map showing the approximate test area (blue rectangle). Background map: Kartverket, c2007

4.1.1 The test area description

Most of the Hardangervidda lies in altitudes above 1000 m a.s.l. , which makes it a mountainous region. However, the terrain is relatively flat. The few exceptions are some valleys and fjords. Probably the most significant are Måbødalen, Hjølmadalen and Simadalen. The only fjord that lies on the images is Eidfjorden. The valley floors are also covered with forests. Furthermore, there are quite a lot of

lakes and bogs in the area, as well as a glacier, Hardangerjøkulen. These special types of land-cover will be masked and treated separately. Several of these lakes are, however dammed and used to produce electricity, so their extent may vary in the radar images and in the land cover map that will be used. The valleys and the fjord will also be accounted for.

The test area is also strongly influenced by the proximity of ocean, as the western part of the area gets significantly more precipitation. Ocean's influence should also result in higher winter temperatures in the western part, as well as it should be noticeable in snow wetness – snow should melt faster in the wetter and warmer parts. A typical winter's week precipitation in this part of Norway is shown in figure 16. It is clearly visible that the precipitation gets stronger as the clouds hit the mountains on the shore and then it gradually weakens. Figure 17 shows a typical seven days average temperature. It is obvious that the temperature drops significantly in the central parts of the Hardangervidda plateau, compared to its eastern part.

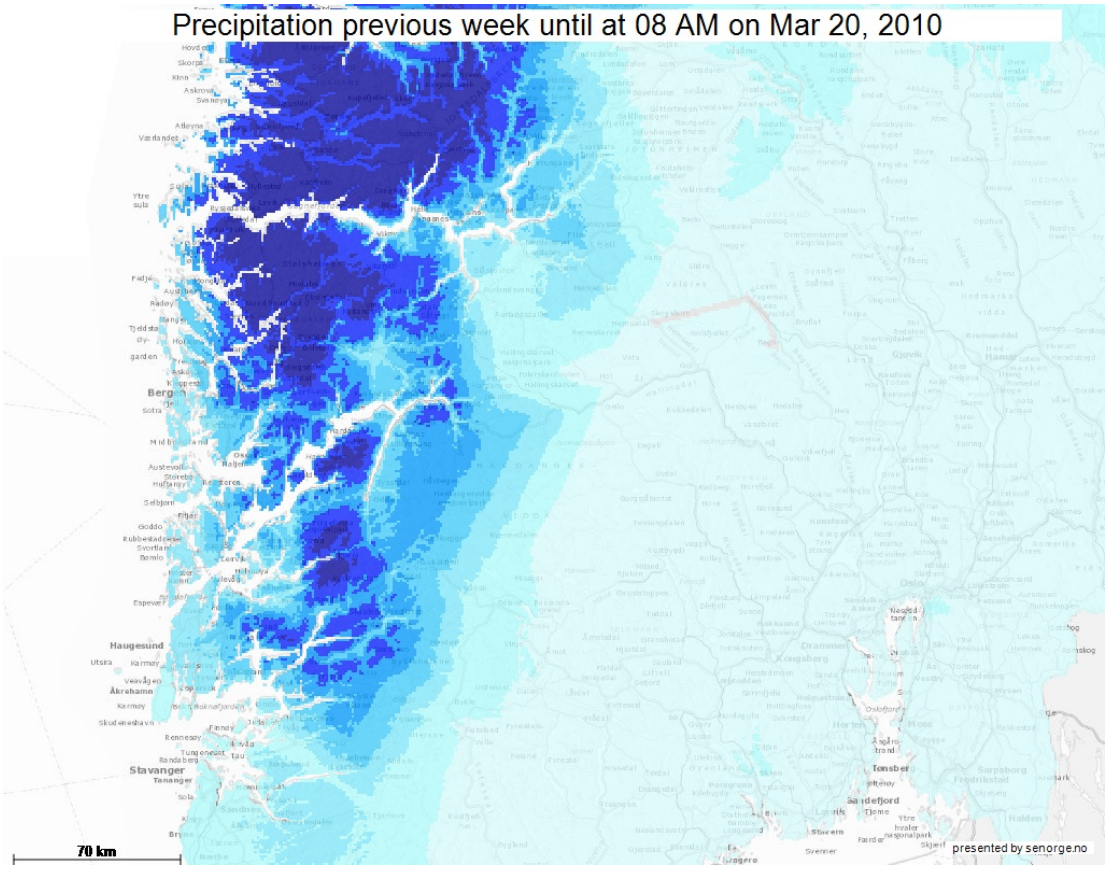

Figure 16: A typical winter week's precipitation over south Norway. Darker blue means more precipitation. Source: NVE (2013?)

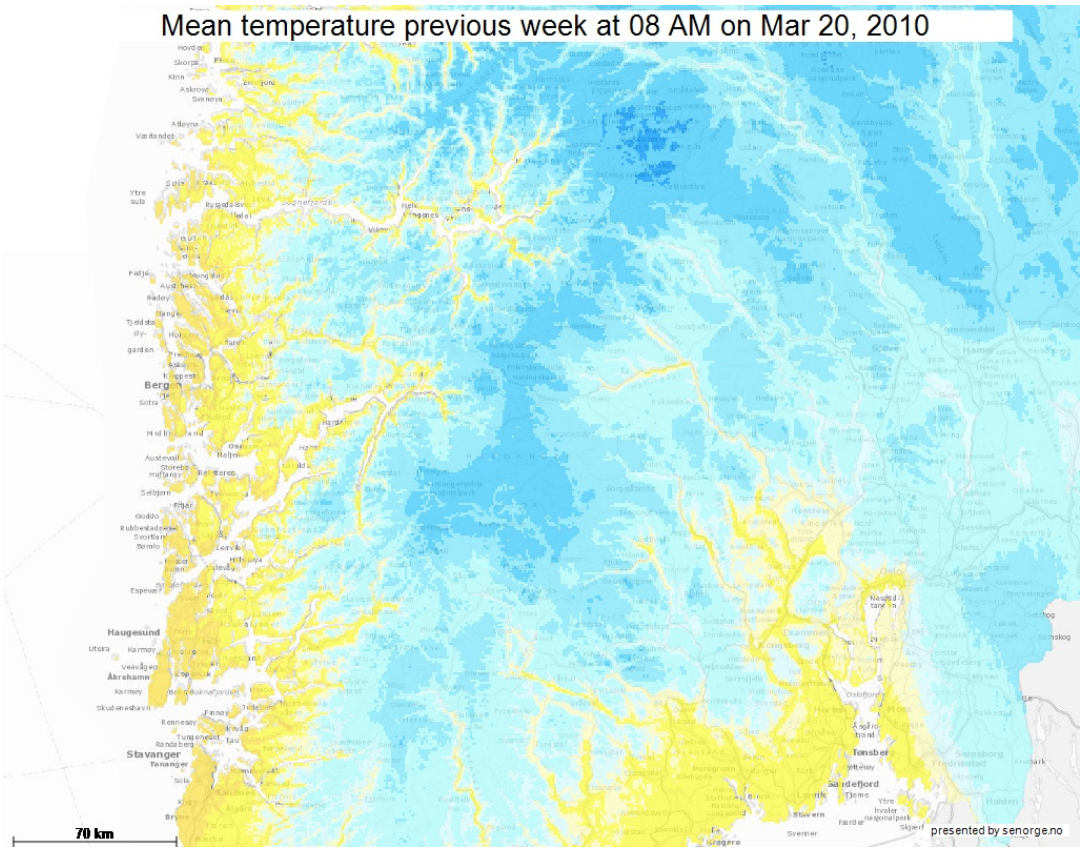

Figure 17: Average temperature over south Norway on a typical winter week. Shades of blue mean temperature below zero and darker means colder. Yellow means temperature above zero. Source: NVE (2013?)

All in all, the test area should provide enough bare ground with low altitude differences. The winter snow cover is also relatively stable here, and, except for the western part of the area and some of the valley floors, only starts melting on spring, so there should not be more freeze-thaw cycles which could cause complicated stratification in the snowpack.

4.2 The satellite images

I have chosen to use data acquired by the ERS-2 mission, mainly because they are relatively easy to achieve for research purposes. Data used in this paper were provided by ESA. The choice of images depended on several factors.

The reference (snow-free) images had to be actually snow-free and, favourably, taken at a time when the soil was relatively dry. The dry soil requirement is important, because wet soil (e.g. soil containing large amounts of water) would have similar backscattering properties as wet snow. Finding images that satisfied both requirements was rather difficult, because Norwegian

mountainous areas are usually not entirely snow-free before September. However, in this period it also rains a lot, so the soil is seldom dry. Furthermore, the first snowfall comes not very long after the last snow has melted. This is the reason why the reference image, taken in July 2010, will still probably contain patches of wet snow.

Nagler and Rott (2000) claim, however, that it is also possible to use images with dry snow cover as reference images. Using dry snow reference images eliminates the risk of wet soil occurring in the reference image. But due to the test area's diversity it was not possible to find an image entirely (or almost entirely) covered by dry snow. There are only a few days every year when the valley floors are covered by dry snow, and the chances of getting a satellite pass on one of the desired tracks during one of these days are very low.

The information about the reference images I have decided to use is summed in Table 5. As mentioned before, the reference image is likely to contain wet snow patches. There has also been some rain the week before each of these images was taken. However, the day before the image was taken, there has only been a little rain recorded over the test area, as seen in figure 18.

It is also important for the reference and test images to have the same imaging geometry, so that the fold mask is the same for both images and the same area is depicted in them

Date	Track	Orbit	Pass
19th July 2010	194	79707	D

Table 5: The reference image information.

Date	Track	Orbit	Pass
13th April 1998	194	15579	D
5th May 2008	194	68184	D

Table 6: The test images information.

The test images were chosen so that they would depict the test area during the snow melt season. I have therefore consulted the ground truth data when selecting these images. The information about the test images is summed up in table 6.

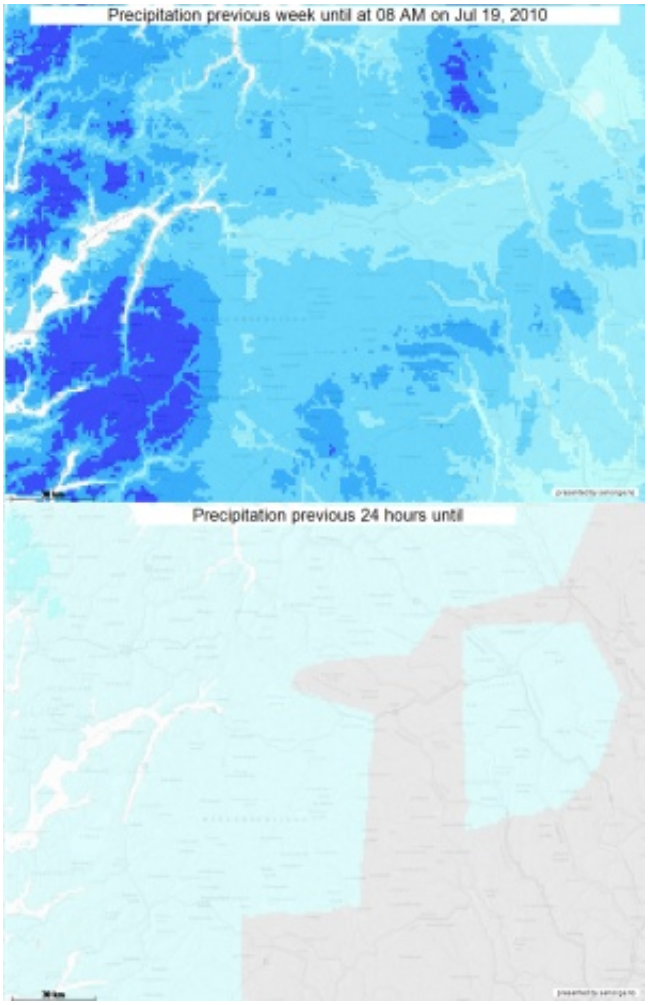

Figure 18: Precipitation over the test area the day/week before each of the reference images was taken. Source: NVE (2013?)

The April image should contain some wet snow, little snow-free ground and some dry snow. So does the May image, but it should contain much less amount of dry snow. These presumptions are based on ground-truth data used while selecting the images.

4.3 Ground-truth data

Ground-truth data concerning snow wetness are very tricky to achieve. Most researchers elect to conduct a field campaign and then wait for data taken during their field campaign. Such a field campaign must, however, be very thorough and it

requires a lot of manpower to collect data from a large area during a relatively short period of time; collecting the data shortly before or after the satellite image acquisition is necessary, because snow wetness may change significantly in less than an hour (see chapter 3), especially in open landscape. Even if I ignore logistical problems (which could be avoided by choosing a different test area), I still lack the necessary manpower and equipment. Not mentioning the fact, that the ERS-2 mission was officially aborted in 2012, when I have barely started working on this paper. Field campaign is therefore out of the equation.

Sometimes optical data can be used, but it requires the optical image to be taken shortly before or after the radar image, and optical images cannot properly distinguish dry and wet snow, so they can only be used to verify the total snow-covered area. However, when it comes to availability, this is probably generally the best option.

Automatic ground measurements of snow wetness are not operationally available in any of the regions I have considered when selecting the test area. Only some automatic measurements of snow depth are available in the test area, which can be used to very roughly compare the modelled and real snow extent. However, such measurements, taken from a single point, are not very reliable – the point where the measurement has been made might be either a part of a small snow-free patch in otherwise compact snow cover, or a small patch of snow in an otherwise snow-free landscape.

However, the NVE has developed a model that computes various hydrological and meteorological statistics in a 1km x 1km grid. All the outputs of this model can be viewed online in a web browser at www.senorge.no and are also accessible via WMS. Altogether the models are called “seNorge” (seeNorway). Obviously, such a model is far from 100% precise, but it has been updated this year and its authors believe that it should be good enough. The old version of the model was subject to an intensive evaluation process (see Stranden, 2010), which helped in the update. After some electronic correspondence with a few NVE researchers, I have decided that this model is the best ground-truth I can get. Especially mr. Tuomo Saloranta has been very helpful, and also confirmed that the data from this model are probably the best choice for this purpose.

Therefore, I will be using data from the seNorge model to evaluate the results achieved in this paper. I also plan using the automatic snow-depth ground

measurements in order to gain as much information about snow extent as possible, but the ground measurements are more of a supplement, and might not prove helpful at all.

4.4 Land cover data

Since radar backscattering may be strongly affected by some land cover categories even when a compact snowpack is present, it is good to handle some of these categories separately. This mostly concerns water bodies, forested areas and bogs and will be discussed further on.

Thanks to the EEA's (European Environment Agency) CORINE (Coordination of Information on the Environment) land cover project, many European countries have performed very detailed land cover mapping. Norway is, luckily, one of these countries and the land cover data were made freely available in vector format by the Norwegian Institute for Forests and Landscape. The smallest area covered in these data is 25 ha, which should be sufficient for the purpose of this paper.

4.5 DEM

A digital elevation model is required for SAR image processing, mainly to account for topographic effects on backscattering. Foreshortening can be corrected, while areas affected by layover and shadow should be masked out. Even though the algorithms used should not be affected by foreshortening, because they employ change detection.

For this purpose, I have purchased a 20 meter grid DEM by Kartverket – Norwegian national cartographic authority. This model should have a standard deviation between 2 and 6 meters and is probably the best option I had for this purpose, due to its combination of acceptable cost and reasonable level of detail and precision.

CHAPTER 5

Methods of wet SCA retrieval from SAR backscattering

5.1 Current methods

Several methods that can obtain information about wet snow-covered area have already been developed. In this paper I will focus on two methods, presented by Koskinen (2001) and Nagler & Rott (2000), which were further improved by Malnes and Guneriussen (2002). All of these algorithms employ change detection to eliminate topographic effects on backscattering.

5.1.1 The Koskinen method

The Koskinen method estimates the fraction of wet snow covered ground and is based on comparing the test image with two reference images. One of the reference images is fully covered with wet snow and the other one is snow-free.

The need for a reference image fully covered with wet snow suggests that this procedure can be hardly used in regions with complicated topography, because in such areas snow wetness can vary significantly on short distances, which would require a large amount of reference images, as each image would only contain a small area with wet snow cover. Koskinen (2001) has tested his algorithm in a rather flat and homogenous area in northern Finland, which is feasible for this method. But the test area used in this paper (see chapter 4) is far from homogenous, as there are strong climatic differences between valley floors and the plateau and also significant differences in climate between east (more continental climate) and west (climate more influenced by the ocean). These phenomena do not occur so strongly on such short distances in Finland.

Furthermore, the Koskinen method is only used to distinguish wet snow from other snow/ground conditions, whereas in this paper I aim to map both dry and wet snow cover. It is, however, a good starting point.

This method uses a linear relationship between backscattering observed in the snow-free reference image and in the wet-snow-covered reference image to calculate the percentage of area covered by wet snow. However, the results are mostly just two classes: wet snow and no wet snow. Just a few pixels contain some intermediate value.

The results of the Koskinen algorithm have been compared to visual observations, which means, that the results presented in his paper are very rough and “only” prove that there is a relationship between the SAR-derived information and field observations. But even this is a success and a good fundament for future research, as well as it shows that probably the most crucial and complicated part of any similar research is obtaining a reasonably detailed and precise ground-truth data set. As I have mentioned before, retrieving ground-truth data requires resources (both financial, technical and human) that most researchers will simply never have.

The same author has also developed an algorithm for snow-melt monitoring in boreal forests (see Koskinen, 2000). This algorithm has been proved to perform reasonably well in modelled conditions. However, it does not take multiple scattering into account, which makes it not feasible for operational use, as well as it does not seem quite fit for use in a paper such as this. I will therefore focus on other land cover classes, as retrieving snow information from forested areas is a very complicated matter by itself.

5.1.2 The Nagler & Rott method

Nagler & Rott (2000) use a simple thresholding algorithm to detect wet snow. They have found that the change in backscattering between the reference image and the wet snow image of -3 dB to be an appropriate threshold for their test area.

Use of images taken from opposite passes has also been suggested in order to obtain information from a larger area. Furthermore, it was Nagler & Rott (2000) that have successfully used an image under dry snow conditions as a reference image. It has also been suggested to use a different classification

approach for different land cover classes, namely agricultural areas that can be affected by surface roughness change, and mires that can be affected by wetness under snow-free conditions. It is either possible to avoid misclassifications on such areas by using land cover maps, topographic information or by studying the seasonal behaviour of backscattering from these areas.

Basically, the decision making of their algorithm is very simple – if a pixel is affected by layover, radar shadow or inappropriate local incidence angles in both passes, then snow mapping is not possible. If not, then the backscattering change between the test image and the reference image is calculated. If the result is less than -3 dB, than the pixel is covered by wet snow, otherwise it is covered by either dry snow or bare ground.

Landsat TM images and photographs taken on the day of the radar pass were used by Nagler & Rott (2000) to verify their results. However, the Landsat data cannot provide proper information on snow wetness. On the other hand, on one of their test images all of the remaining snowpack was supposedly wet. Overall, they have achieved 83% agreement between the ERS and Landsat images.

Temporal consistency of SAR-derived snow maps was also investigated by Nagler & Rott (2000). It was based on the assumption, that pixels once classified as snow-free should remain snow-free later in the season, in case no fresh snow falls. A pixel by pixel comparison showed that 3.2 % of pixels classified as snow-free in June were classified as wet snow in July. This inconsistency is said to might have been caused by level of multi-looking and speckle filtering or by inaccurate geocoding and coregistration.

5.1.3 The Malnes method

Malnes and Guneriussen (2002) have based their research on the two methods mentioned previously. The result of their work is a sub-pixel classification of wet snow, which, together with a reasonably detailed DEM, can also detect dry snow. For simplicity's sake, I will refer to their algorithm as to the "Malnes' algorithm" from now on.

Malnes' algorithm masks out forest and water, because these two land cover classes give ambiguous results in SCA mapping. Also pixels affected by

shadow or layover are masked out. The remaining pixels are than classified using modified Nagler's & Rott's (2000) algorithm. Resulting classification classes are snow-free ground, pixels containing 0 – 100 % of wet snow and dry snow.

The technique employed to obtain percentage of wet snow cover in a pixel originates from the -3 dB classification threshold found by Nagler & Rott (2000) and the linear sub-pixel classification scheme used by Koskinen (2001). Malnes and Guneriussen (2002) have, however, found, that using a "soft" threshold centered around -3 dB together with the sigmoid function shown in formula 5 (*x* being the backscatter and *a* being a slope parameter for the function – see figure 19) gives more information than the "hard" threshold used by Nagler & Rott (2000). The percentage of wet snow cover on each pixel is derived from the sigmoid function. Figure 19 shows the sigmoid function used for sub-pixel classification.

$$\mathbf{5}: F(x) = 50 - 50\tanh[a * (x + 3)]\ \%$$

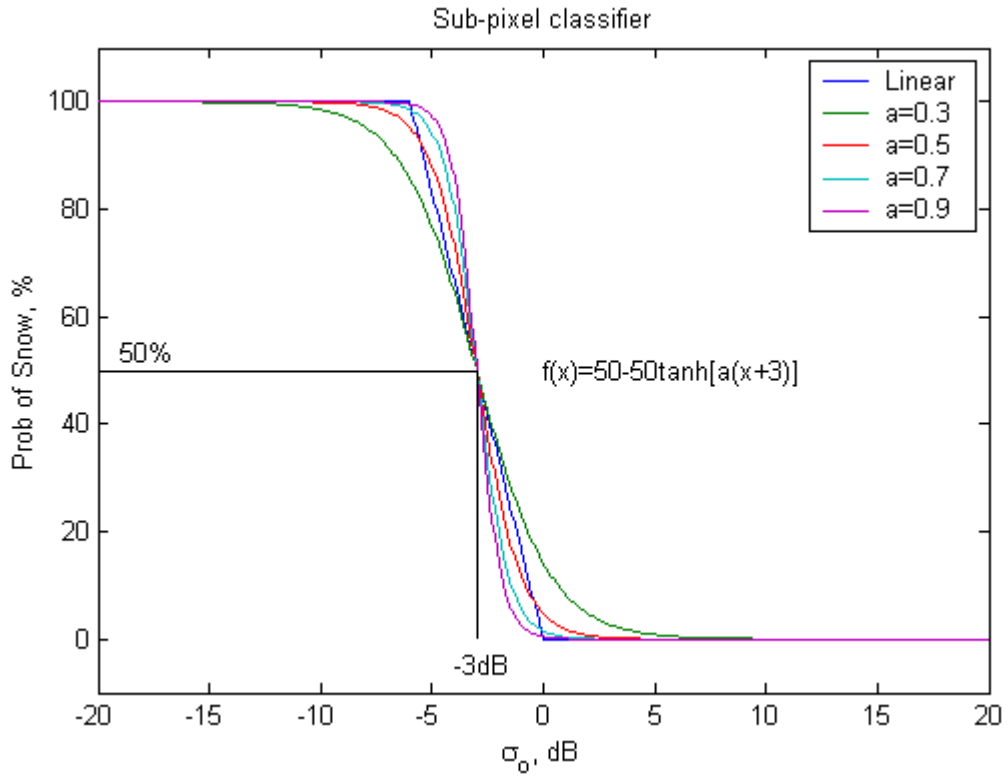

Figure 19: Weight function for sub-pixel classification of wet snow. When the difference is below 0 dB, snow is classified as 0 – 100% wet. Source: Malnes and Guneriussen (2002)

Another improvement of Malnes' algorithm is, that after performing the wet snow classification, it is possible to postulate that all pixels that lie above the median altitude of wet snow and that are not classified as wet snow, can be classified as dry snow. This is applicable in Norwegian mountains, but does not

have to apply in other regions, like the Alps, where mountain tops may be snow-free due to wind (Malnes and Guneriussen, 2002)

Malnes and Guneriussen (2002) have also suggested a special classification scheme for water bodies and suggest that other land uses can be processed in a similar manner. In this paper, I will attempt to process water bodies separately.

Statistical methods have been used by Malnes and Guneriussen (2002) to calculate the error rate achieved by their algorithm, because the authors were not able to find any suitable optical images. The resulting overall error rate was computed to be 16.6 % (see figure 20).

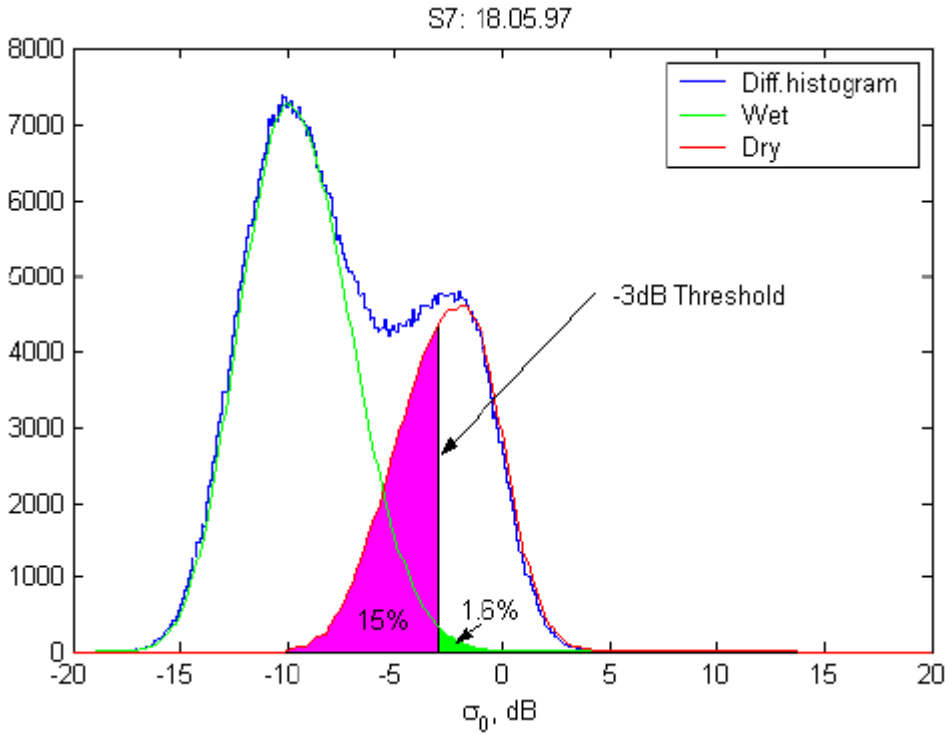

Figure 20: Error assessment. The difference image histogram is fitted with two distributions, representing wet snow and dry snow/bare ground. Error rates are calculated by estimating the areas below the respective curves from the threshold. Source: Malnes and Guneriussen (2002).

5.2 The method used in this paper

For the purpose of this paper, I will be testing the Malnes' algorithm (see previous chapter) and see if I can achieve better results by applying a different classification scheme for open water bodies. As I have previously suggested, the most favourable limit for wet snow to be monitored is 2 % of volumetric wetness. Wet

snow will in this paper be considered snow containing more than 2 % of liquid water.

I have decided not to use any radiometric corrections, as they could affect the result. I think it is best to keep the data as close to what was recorder by the sensor as possible. Only the necessary calibrations will be performed, and afterwards topographic effects will be corrected and a mask of areas affected by shadow and layover will be prepared.

After the images are prepared, areas affected by shadow and layover will be masked out. Then, water and forest classes will be masked out and the rest of the image will be classified as done by Malnes and Guneriussen (2002). Afterwards, a classification algorithm (see further) will be applied on water pixels. I have also originally planned to try and use an optical image taken within a short period of time before or after one of the radar images, to improve classification accuracy in areas not obscured by cloud cover. However, it was not possible to find a suitable optical image for this purpose, so I will only present the algorithm suggestion further in this paper.

5.2.1 Water classification algorithm

The algorithm for classification of snow cover over water bodies, suggested by Malnes and Guneriussen (2002), relies on detecting seasonal changes in backscattering. A dry snow cover on top of ice means higher backscattering than open water. Wet snow cover on top of ice will result in backscattering reducing to about the same level as open water. Snow-free ice will have higher backscattering than open water and backscattering from open water is low. If this algorithm is used on a series of images, it is easy to follow the changes in backscattering and determine if the pixel contains dry or wet snow, ice or open water.

But for a single image, when there is no possibility to compare the current image with other images taken earlier or later in the season, the classification gets tricky. Because the backscattering from dry snow and snow-free ice is more or less the same, and so is the backscattering from open water and wet snow.

I will therefore use a change detection algorithm that will have two phases. In the first phase, change from the reference image (that contains open water), will be detected. A sub-pixel classification scheme similar to that used for detecting wet

snow will be used, except that the “soft” threshold will be centered at 3dB, instead of -3 dB (when detecting wet snow on ground, we are looking for decreased backscattering, while when detecting ice and dry snow on lakes, we are looking for an increase in backscattering). The classification function is shown in formula 6.

$$\mathbf{6}: F(x) = 50 + 50\tanh[a * (x - 3)]\ \%$$

The first phase of the algorithm leaves us with the information that the pixel is covered with a certain percentage of either dry snow/snow-free ice or wet snow/open water. Each of the two possible classes for each backscattering possibility (low or high) represents a “warm” or “cold” weather case. This is summed in table 7.

	Warm weather	**Cold Weather**
Low backscattering	Open Water	Wet Snow
High backscattering	Snow-free ice	Dry snow

Table 7: Snow detection on water bodies. Low backscattering means backscattering roughly the same as in the reference image, while high backscattering means backscattering higher than reference image.

Therefore, the problem now is to determine whether we have a warm or cold weather case. This could be done by similar means as estimating dry snow. But because water bodies are most commonly found on valley floors and other low-altitude locations, using the median altitude of pixels classified as wet snow, would probably not work properly. What we are interested in, is what snow condition is the most common in pixels near the water body. Therefore, a buffer zone around the water body will be established, and the most common value in this buffer zone will be found.

If the most common value in this buffer tone is dry snow, then we have the cold weather case. If bare ground is the most common, than we have the warm weather case. If wet snow is the most common value in the buffer zone, it is possible that the high backscattering pixels are covered by either ice or dry snow. Therefore, we have some sort of intermediate weather case. After some experimenting, it seems that the best way to deciding this, is finding whether there is more dry snow or bare ground in the buffer zone.

From here, there are three possible cases. If there is more dry snow than bare ground in the buffer zone, than high backscattering pixels should be classified as dry snow . Otherwise, if there is more bare ground than dry snow, or if there is only wet snow in the buffer zone, high backscattering pixels should be classified as snow-free ice

The appropriate size of the buffer zone depends on the area. We want to get information from as many pixels as possible, but at the same time, we need to only consider pixels with climatic conditions similar to those of the water body. Also, the pixels that are closest to the water body's boundaries will probably contain some mixed values. The pixel size in an ERS image is 25 x 25 meters. I have found a 200m buffer zone to be appropriate, as the snow properties should not change much on a 200m distance in the test area.

It is also important to remember, that climate may change significantly on relatively short distances and that local differences in climate will, for obvious reasons, affect the results of this classification algorithm. Therefore, the lakes should be classified either one by one, or in groups that have similar climate conditions.

5.2.2 Improving classification accuracy with optical data

Distinguishing snow from other land cover classes in optical images is fairly easy. The only thing that may be misclassified as snow are clouds. However, cloud covered areas can be easily identified and masked out. As mentioned in chapter 3.5 of this paper, at wavelengths above around 1,5 μm the reflectance of snow cover drops significantly, while the reflectance of clouds remains very high.

Therefore, the extent of snow cover could be first determined from an optical image and then classified as either wet or dry using SAR data. The first step would be classifying the optical image into three classes: snow cover, cloud cover and other. Then all SAR pixels lying in the area that was classified as "other" in the optical image will be classified as bare ground. All remaining pixels will be classified using the Malnes and Guneriussen (2002) algorithm, including classifying dry snow pixels. Afterwards, SAR pixels that have not been classified as either dry, or wet snow, and lie in the optical data snow mask, will be classified as dry snow.

This way there are no bare ground pixels in the optical data-derived snow mask. Pixels lying in the cloud mask would not be reclassified using the optical data.

This algorithm should significantly reduce misclassifying bare ground as snow and vice versa in areas not obscured by cloud cover. Given that classification of snow using optical data should be very reliable, this should improve the overall accuracy of a snow classification algorithm.

Unfortunately, I have not been able to achieve any suitable optical data for testing this algorithm, so it only remains a proposition for the time being.

CHAPTER 6

Results & Discussion

6.1 The wet snow classification algorithm

Two satellite images have been processed and classified using the Malnes' algorithm. Two classifier parameter values have been tested: 0.5 and 1 (linear classifier). The resulting rasters display pixels classified as bare ground or dry snow and pixels containing a percentage of wet snow and bare ground/dry snow.

The resulting map of snow cover on 13th April 1998 is shown in figure 21. This is the more interesting of the two classified images, as this map actually contains some distinguishable areas of wet and dry snow. Figure 22 shows the snow wetness map as modelled by NVE.

Even though both maps are different at first glance, there are some trends that suggest that the classification scheme is not far from reality. When evaluating the two maps, it is important to bear in mind the massive difference in spatial resolution between the two products. Around Bjørnesfjorden lake (marked with number 1) we can see an area covered in dry snow. This area of dry snow ends in the north-east near lake Sysenvatnet (marked number 2) and in the south in two valleys near lake Songavatnet (marked number 3). The dry snow area in the SAR-derived map is not consistent, unlike the one produced by the model, which may be accounted to the coarse spatial resolution of the model. Also, the SAR product contains a lot of pixels that have been classified differently from their most frequent neighbours. This might have been caused by speckle in the SAR image. However, using a stronger speckle filter would change the original values more significantly and could affect the overall classification results. Another way to get rid of this phenomenon would be generalizing the classified raster.

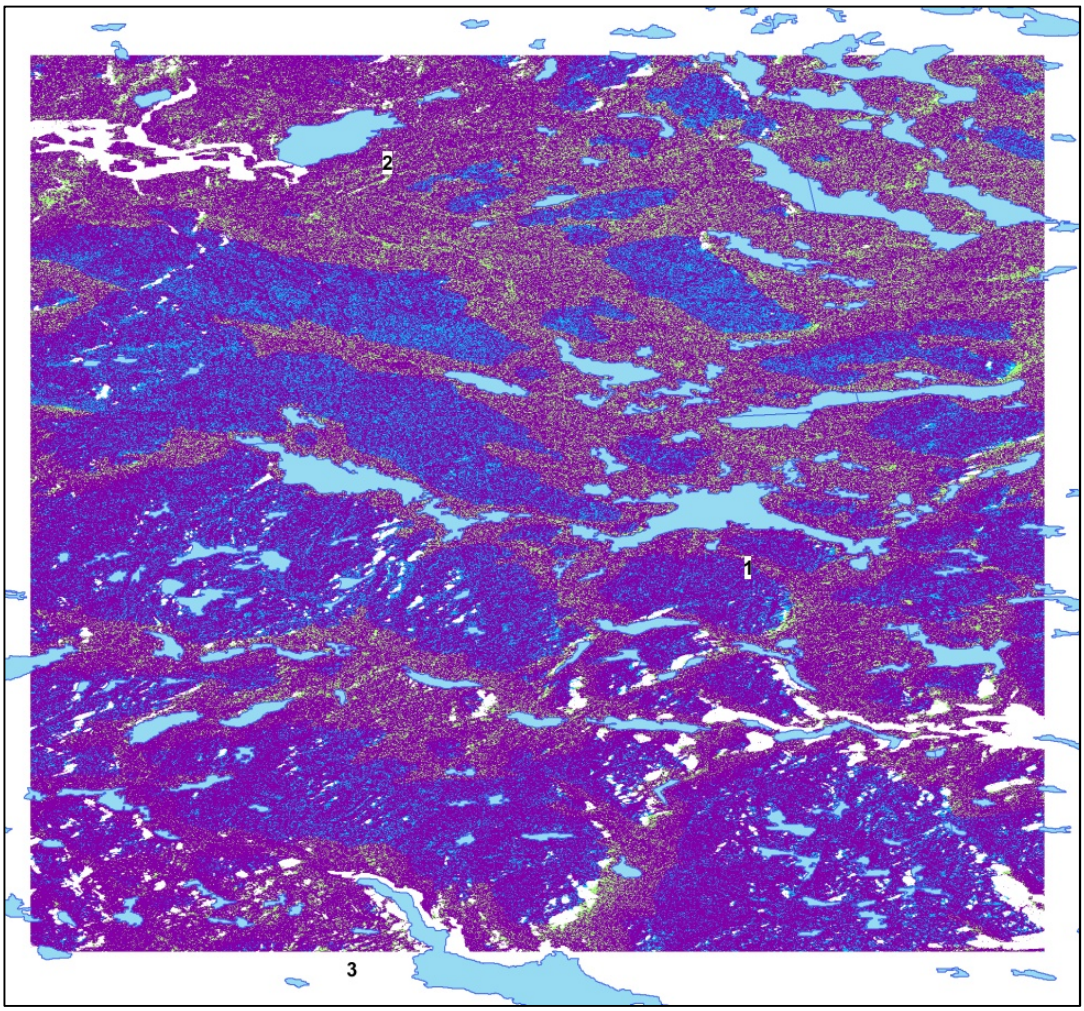

Figure 21: SAR derived snow cover map for 13th April 1998 with a water layer added for easier orientation. 1 – Bjørnesfjorden lake. 2 – Sysenvatnet lake. 3 – Songavatnet lake.Blue pixels represent dry snow, purple pixels wet snow and green pixels bare ground.

The situation on 5th May 2008 was very different. Even according to the NVE model, most of the test area was covered by wet snow. The SAR-derived map contains hardly any pixels of other class (see figure 23). In the NVE model output we can see some patches of dry snow. This might be due to the model‘s tendency to slightly overestimate snow cover, mentioned by mr. Tuomo Saloranta in one of his e-mails.

However, it is more likely to have been caused by the classifier itself. Because it determines that a pixel contains a certain percentage of wet snow, but does not say whether the remaining area of the pixel is bare ground or dry snow. It may therefore be a good idea to find a way to also classify the other part of the pixel. Another possible way is to only classify pixel as wet if it contains more than, for example, 50 % of wet snow. Otherwise the pixel could be classified in the same

way as pixels not containing wet snow are, to decide if the other part of the pixel is covered by bare ground or dry snow.

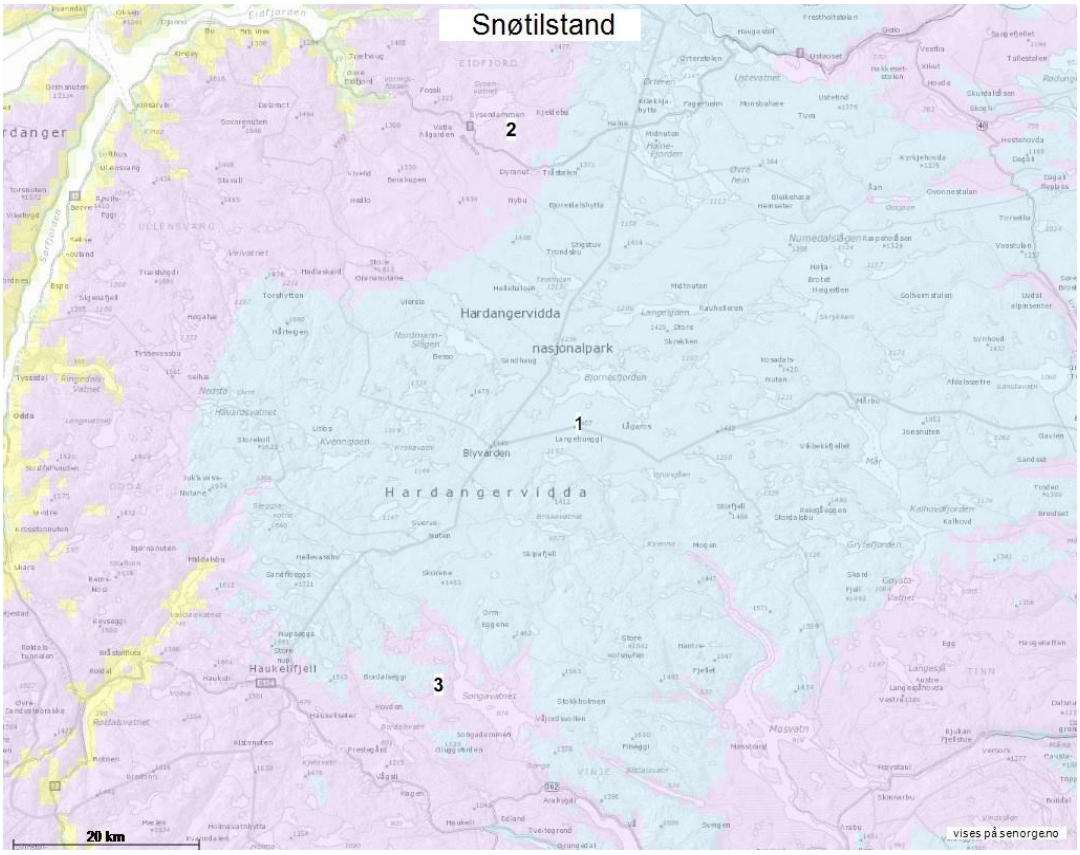

Figure 22: Snow cover map for 13th April 1998 with a water layer added for easier orientation. 1 – Bjørnesfjorden lake. 2 – Sysenvatnet lake. 3 – Songavatnet lake.Blue pixels represent dry snow, purple pixels wet snow and green pixels bare ground. Source: NVE (2013?).

To confirm the idea that most of the wrongly classified pixels contain less than 50% of wet snow according to the classifier, I have generated 20 random points over the two rasters, and for each point compared the most frequent value in its 75 m buffer zone with the value found on the same coordinates in the NVE model. Unfortunately, because the WMS provided by seNorge is not queryable, this had to be done manually on seNorge's website. The results of this effort are presented in table 8.

According to the data in table 8, the 2008 image was classified with 95% accuracy. The only misclassification was a point that was surrounded mostly by pixels classified as containing more than 50 % of wet snow, but contained dry snow according to the model. So, this one does not support the theory, that misclassified pixels contain less than 50 % of wet snow. However, in the other image, all test points were surrounded mostly by pixels containing less than 50 %

of wet snow. And 85 % of them contained dry snow according to the model. After examining each of the test point's surroundings in the SAR-derived map, I learned that very often the second most frequent value was dry snow. This suggests that the pixels might have been correctly classified as to the content of wet snow in them, but the dominant part of the pixel was actually covered by dry snow.

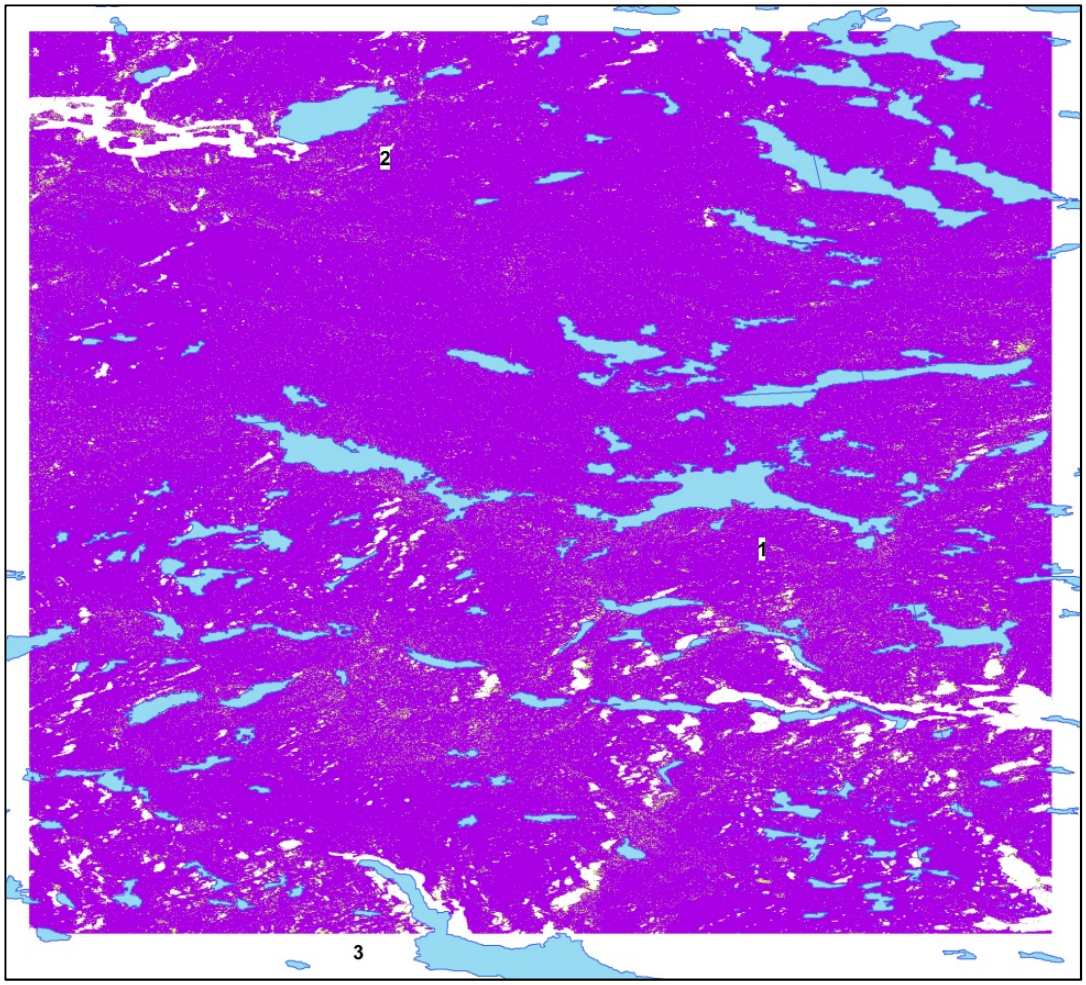

Figure 23: SAR derived for snow cover map 5th May 2008 with a water layer added for easier orientation. 1 – Bjørnesfjorden lake. 2 – Sysenvatnet lake. 3 – Songavatnet lake.Blue pixels represent dry snow, purple pixels wet snow and green pixels bare ground.

These results then lead to the need of classifying the other part of pixels that contain less than 100 % of wet snow. And especially pixels that contain less than 50 % of wet snow, because it is the most frequent type of snow cover that is of interest. As suggested before, this could be done by employing the same algorithm that classifies pixels with no wet snow. It is very unlikely that an area of 25 x 25 meters could contain dry snow, wet snow and bare ground at the same time, so I think it is safe to presuppose that the pixel will only contain two classes of snow

cover. The most interesting part in this, is finding the type of snow cover that contributes the most to the total backscattering from a pixel.

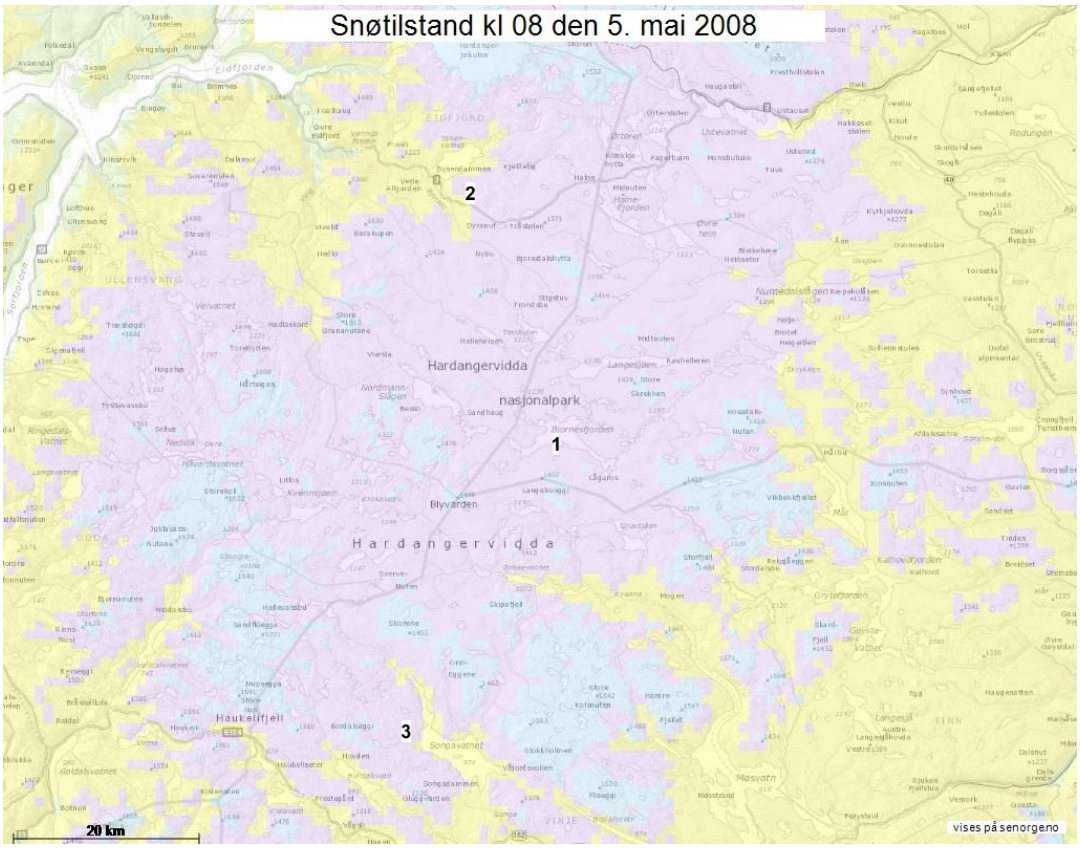

Figure 24: Snow cover map for 5th May 2008 with a water layer added for easier orientation. 1 – Bjørnesfjorden lake. 2 – Sysenvatnet lake. 3 – Songavatnet lake.Blue pixels represent dry snow, purple and yellow pixels wet snow and green pixels bare ground. Source: NVE (2013?).

Various values of the parameter *a* in the classification formula have been tested. The overall results did not vary significantly based on this parameter. However, in some cases it may make sense to adjust the parameter value. Values closer to 1 will produce more pixels classified as no snow or 100 % wet snow. When we only have a couple of pixels classified as 100 % wet snow in the entire image, we can hardly consider the median altitude computed from these few pixels reliable, so it may be a good idea to adjust the parameter value in order to use get more pixels classified as 100% wet snow.

Point	20080505	real 20080505	19980413	real 19980413
1	> 50% wet	wet	**< 50% wet**	**dry**
2	< 50% wet	wet	< 50% wet	wet
3	> 50% wet	wet	< 50% wet	wet
4	> 50% wet	wet	**< 50% wet**	**dry**
5	> 50% wet	wet	**< 50% wet**	**dry**
6	< 50% wet	wet	**< 50% wet**	**dry**
7	> 50% wet	wet	**< 50% wet**	**dry**
8	> 50% wet	wet	**< 50% wet**	**dry**
9	> 50% wet	wet	**< 50% wet**	**dry**
10	< 50% wet	wet	**< 50% wet**	**dry**
11	> 50% wet	wet	**< 50% wet**	**dry**
12	> 50% wet	wet	**< 50% wet**	**dry**
13	**> 50% wet**	**dry**	**< 50% wet**	**dry**
14	> 50% wet	wet	**< 50% wet**	**dry**
15	< 50% wet	wet	**< 50% wet**	**dry**
16	> 50% wet	wet	**< 50% wet**	**dry**
17	> 50% wet	wet	< 50% wet	wet
18	> 50% wet	wet	**< 50% wet**	**dry**
19	> 50% wet	wet	**< 50% wet**	**dry**
20	> 50% wet	wet	**< 50% wet**	**dry**

Table 8: Random points compared to ground truth.

6.2 The snow on water bodies classification algorithm

An algorithm for classifying snow cover on lakes, proposed in chapter 5, has been tested. Unfortunately, no useful ground truth data are available for such a task, so the results of such algorithm cannot be confirmed otherwise than by a field campaign or optical data.

In figure 25 there is a classified image of snow on water bodies, derived from the 1998 SAR image. The most common value in the buffer zones in this case was bare ground, which means that red colour indicates open water and blue indicates snow-free ice. Figure 26 depicts the same map derived from the 2008 SAR image. The most common value in this case was wet snow and there was more bare ground in the buffer zones than there was dry snow. This means that red colour indicates wet snow and blue colour snow-free ice.

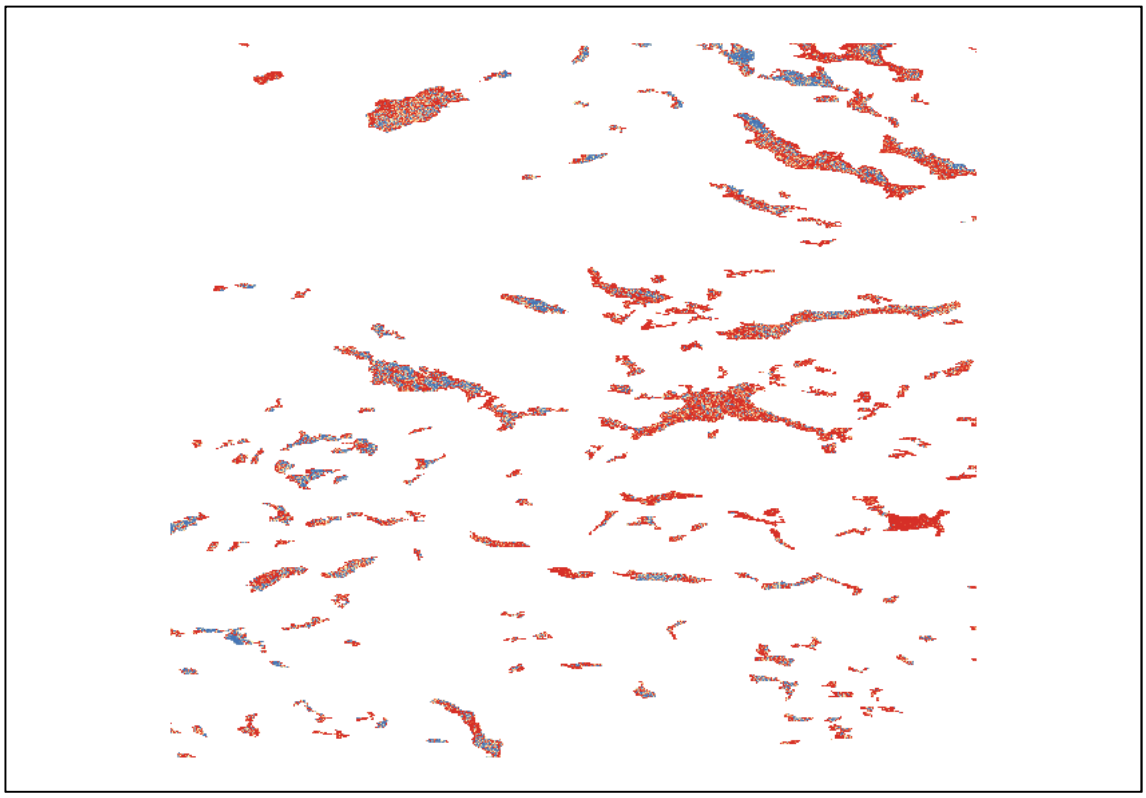

Figure 25: SAR derived snow cover on lakes on 13th April 1998.

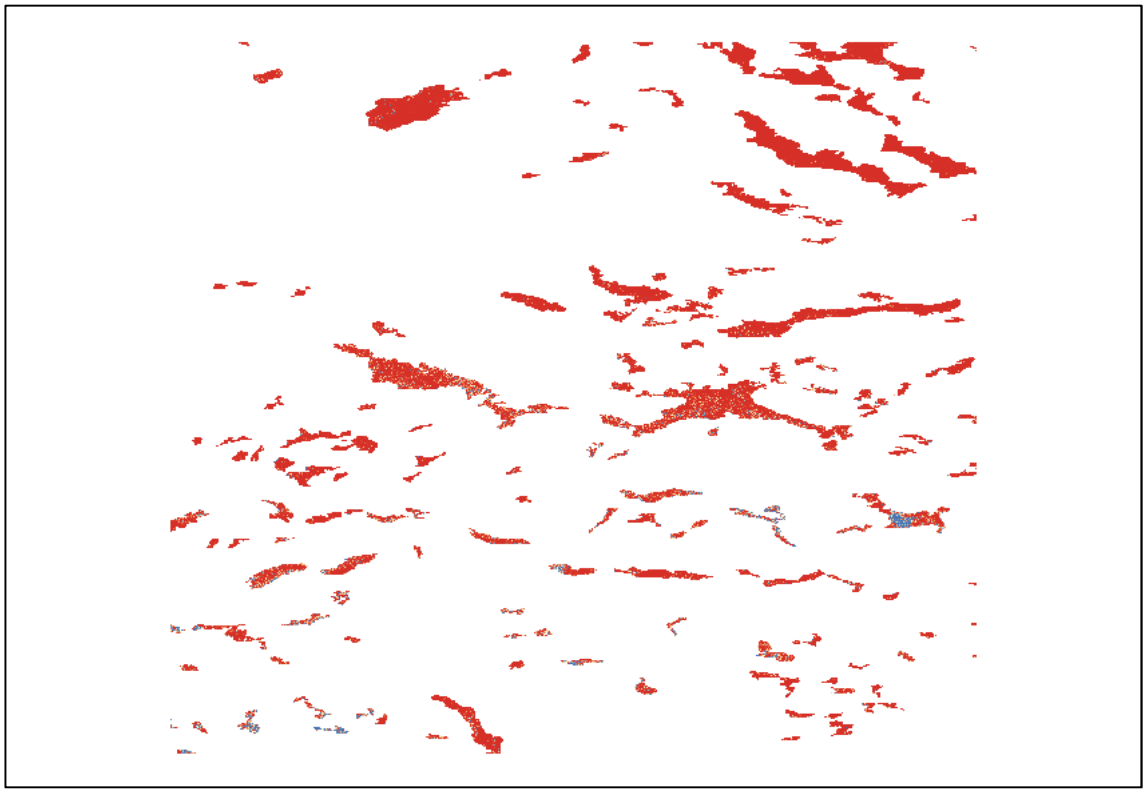

Figure 26: SAR derived snow cover on lakes on 5th May 2008.

The fact that the April image contains water and ice and May image contains wet snow and ice may wake suspicions regarding the algorithm's reliability. On the

other hand, these images were taken 10 years apart of each other, so the classification does not necessarily have to be wrong, as the two winter's could have been entirely different.

Nevertheless, further work is needed on this topic. Also, for example wind speed should be taken into account, as it may significantly change backscattering from water. This problem could be reduced by carefully choosing the reference image from a day with little or no wind, but it will persist in the test images if they contain open water too.

6.3 Using optical data for improving classification accuracy

An algorithm for improving the accuracy of Malnes' (2005a) algorithm when optical data are available, has been proposed. Unfortunately it was not possible to test it, due to lack of suitable data. I therefore cannot draw any conclusions regarding this matter, I can only encourage further research on this topic. The proposed algorithm is described in a flow chart in figure 27.

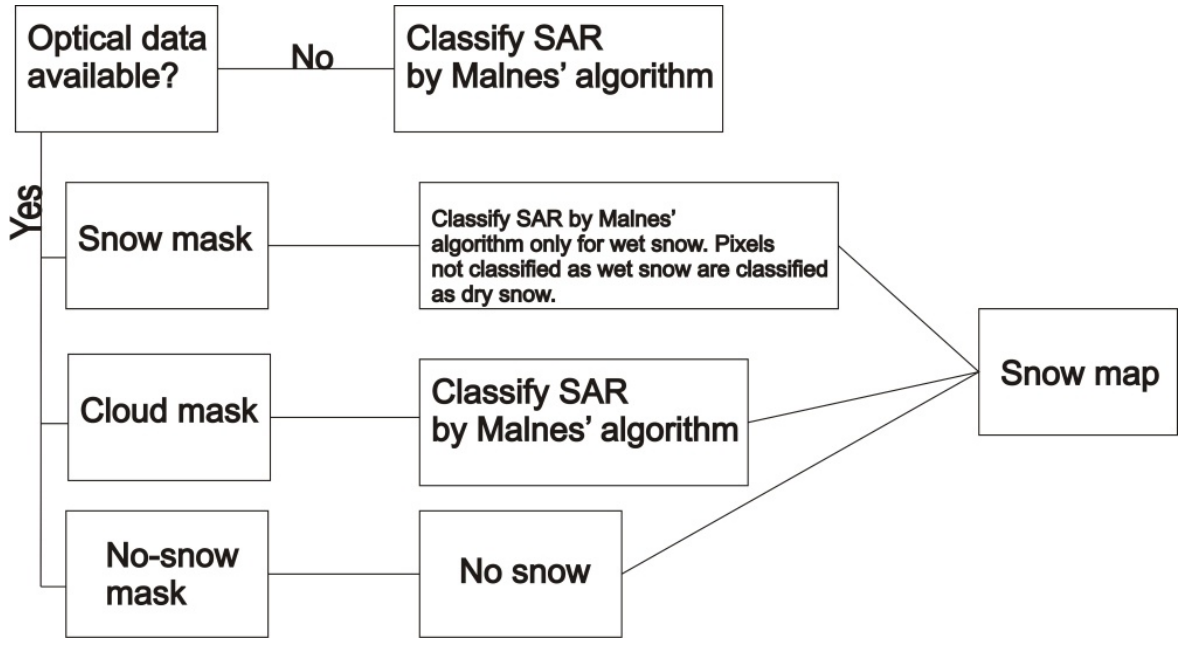

Figure 27: A flow chart of the proposed classification algorithm.

CHAPTER 7

Conclusion

The Malnes' algorithm has been tested on a set of two images and the results were compared with modelled data, which were used as ground truth. The algorithm's weakest spot seems to be the fact, that it does not determine what covers the remaining part of a pixel, that has been classified as a pixel that contains a certain percentage of wet snow. Due to this, many pixels that, according to the algorithm, contain less than 50 % of wet snow, have been misclassified, because they were marked as wet snow, regardless of what type of snow cover makes the dominant part of the pixel. When classifying snow, it is better to know what contributes most to the total backscattering, even though a sub-pixel information is always neat. A possible solution has been proposed to handle this problem.

To improve the total classified area and enhance the ability of the SCA retrieval algorithm, an algorithm for classifying snow cover on frozen lakes has been proposed and tested. It was not possible to achieve suitable ground truth data to verify the results.

Finally, a way to improve classification accuracy using optical data has been proposed. Due to lack of access to suitable data, it was not possible to check how it would affect the results, but I believe that optical data can identify snow more reliably than radar data, as long as they are available and not obscured by cloud cover. I therefore think that a multi-sensor approach could improve the overall accuracy of snow cover classification.

REFERENCES

DOPROVOLNÝ, P. 1998. *Dálkový průzkum Země. Digitální zpracování obrazu.* Brno, Přírodovědecká fakulta Masarykovy univerzity, Katedra geografie. ISBN 80-210-1812-7.

DOLEŽAL, E., POLLAK, T. 2004. *Vlastnosti sněhu* [online]. [quoted 2013-05-20]. Available from URL: <http://ekologie.upol.cz/ku/mat/zhoek>.

ENGEN, G. et al. 2003. *New approach for Snow Water Equivalent (SWE) estimation using repeat pass interferometric SAR*. Proceedings IGARSS03, Toulouse, France, July 2003

ESA. [c2013]. Synthetic aperture radar. *Earthnet Online* [online]. [quoted 2013-03-12]. Available from URL: <http://earth.esa.int/applications/data_util/SARDOCS/spaceborne/Radar_Courses/Radar_Course_II/synthetic_aperture_radar_SAR.htm>

FERRETTI, A. et al. 2007. *InSAR Principles: Guidelines for SAR Interferometry Processing and Interpretation.* The Netherlands, European Space Agency

FINSLAND, W. 2007. *Vurdering av mulighetene for kartlegging av snøskred med fjernanalyse*. Master's thesis. Oslo, University of Oslo.

KARTVERKET. [c2007]. *Topografisk Norgeskart 2 WMS service*. [WMS Service]. Available from URL: <http://openwms.statkart.no/skwms1/wms.topo2?>

KLEIN, A. G. et al. 1998. Improving snow cover mapping in forests through the use of a canopy reflectance model. *Hydrological processes*. No. 12.

KOLÁŘ, J. et al. 1997. *Dálkový průzkum Země 10*. Prague, Vydavatelství ČVUT. ISBN 80-01-01567-X.

KOSKINEN, J. et al. 2000. Effect of snow wetness to C-band backscatter - a modelling approach, *Report 4 Laboratory of Space Technology,* Helsinki University of Technology, Espoo. Available from URL: <https://aaltodoc.aalto.fi/bitstream/handle/123456789/2318/article5.pdf?sequence=6>

KOSKINEN, J. 2001. *Snow monitoring using microwave radars*. Helsinki, 2001. Thesis for the degrese of Doctor of Technology, Helsinky University of Technology.

MALNES, E., GUNERIUSSEN, T. 2002. Mapping of snow covered area with Radarsat in Norway. *Proceedings to IGARSS, Toronto, Canada, 24-28.june, 2002*. Available from URL: <http://projects.itek.norut.no/EnviSnow/Publications/Malnes_Earsel_2002.pdf>

MALNES, E. et al.2004. *EnviSnow - Radar remote sensing of snow water equivalent (SWE)*. Available from URL: <http://projects.itek.norut.no/EnviSnow/D07_SWE_report_v1.0.pdf>

MOEN, J., LANDMARK, B. 2008. *Satellittbasert miljøovervåkning*. Tromsø: Eureka Digital. ISBN 978-82-7389-135-8.

NAGLER, T., ROTT, H. 2000. Retrieval of wet snow by means of multitemporal SAR data. *Geoscience and Remote Sensing, IEEE Transactions on*. Vol. 38, No. 2.

NVE. *NVE's snow pillow station* [online]. [c2007]. Available from URL: <http://www.nve.no/PageFiles/11073/prinsippskisse-av-snopute.pdf>

NVE. 2008. *Retningslinjer for hydrologiske undersøkelser: Retningslinjer for manuelle målinger av snø samt innsending av data til Norges vassdrags- og energidirektorat (NVE)* [online]. Available from URL: <http://www.nve.no/Global/Sikkerhet%20og%20tilsyn/Milj%C3%B8tilsyn/Hydrologiske%20p%C3%A5legg/15_Snomaling.pdf>

NVE. 2009. Satelittfjernmåling. *Norges vassdrags- og energidirektorat* [online]. [quoted 2013-04-25]. Available from URL: <http://www.nve.no/no/Vann-og-vassdrag/Hydrologi/Sno/Satelittfjernmaling/>

NVE. [2013?]. Senorge.no. *Senorge.no* [online]. [quoted 2013-05-04]. Available from URL: <http://www.senorge.no/>

ROGNES, A. et al. 2005. Satellite based snow monitoring for hydropower production and trade in Norway – results versus operational needs. *Proceedings to ISRSE, St. Petersburg, Russia, June 2005.* Available from URL: <http://publications.nr.no/4060/Rognes_-_Satellite_based_snow_monitoring_for_hydropower_pro.pdf>

ŠPÁTOVÁ, Z. 2010. *Využití dat dálkového průzkumu Země pro určování vodní hodnoty sněhu.* Master's thesis. Prague, Charles University in Prague, Faculty of Science.

STRANDEN, H.B. 2010. *Evaluering av seNorge: data versjon 1.1.* NVE. Available from URL: <http://www.nve.no/PageFiles/11067/dokument4-10.pdf>

STORVOLD, R. et al. 2006. SAR remote sensing of snow parameters in Norwegian areas - current status and future perspective. *J. of Electromagn. Waves and Appl.* Vol 20, No. 13.

APPENDIX LISTING

Appendix 1 CD